1

Introductory Concepts

Components and Design Issues for a Multigigabit Link over Multimode Fiber

1.1 Introduction

The recent huge demand for Multigigabit Ethernet (10GbE) and Fiber Channel (FC) standard applications in metropolitan areas has very rapidly pushed up the need for broader modulation frequency ranges in deployed multimode optical fibers. Since the beginning of the Gigabit Ethernet (GbE) in 1997, a great effort has been devoted to qualify transmission performances of standard multimode fiber (MMF) deployed in buildings, offices and everywhere around metropolitan areas. Multimode fibers had been developed in the past 20 years and an increase in optical fiber manufacturing and very different manufacturing procedures led to a very different transmission behavior and modal bandwidth optimization. At the beginning of the optical fiber transmission era, about 30 years ago, multimode fibers were deployed for use with light emitting diodes (LED) and low-bit-rate-based optical links, usually operating below 200 Mb/s. Since the advent of the Gigabit Ethernet during the late 1990s, the expected bit rate today has increased demand for multigigabit Internet routing in the metropolitan area, but this may not be possible due to the inherently slow transmission properties of the deployed multimode optical fibers. The transmission speed is no more than 1 Gb/s but 10 Gb/s and beyond are today requested for MMF links from most of the service providers.

Most of the installed multimode fiber base was manufactured during the 1980s and early 1990s, when the multimode optics was conceived essentially for subgigabit transmission applications, using surface emitting LED and large area PIN diodes operating mainly at 850 nm. High-speed optical transmission was concentrated on single-mode fiber technology where high transmission capacity easily allowed 10 Gb/s transmission over several tens of kilometers. High-speed telecommunication was concentrated mainly in the backbone market, where huge transmission capacities were needed to link large and faraway metropolitan areas. As soon as the Internet started to grow more quickly in the local area network, there was a need to increase the transmission capacity of the existing fiber infrastructure. That layout was structured with multimode fiber of use only for previous low-speed applications and the need for new engineering challenges in utilizing deployed multimode fibers at 10 Gb/s appeared as one of the major tasks facing the datacommunication industry. Efficient light sources such as the vertical cavity surface emitting laser (VCSEL) are suitable candidates for high-speed direct modulation, but they require new investigations on the effect of launching conditions

on multimode fiber propagation behavior. The conventional multimode fiber coupling technology must be revised to take account of the new laser launching and multigigabit data rate, including fusion splices, connectors and optical couplers. Because of the complexity and the relevance of these applications, the new standard 10BASE-LRM is under development by the IEEE802.3ae committee.

1.2 Multimode Optical Fibers

Optical fibers have been widely deployed to serve extremely high performing transmission channels for both telecommunication and datacommunication applications since their first industrial manufacture in the mid seventies. For almost thirty years, optical fibers have represented the best transmission channel technology available for either long-reach backbone transmission or large local area distribution purposes. In order to serve a multigigabit transmission medium every wired transmission channel should have simultaneously low attenuation and high bandwidth per unit length. Optical fiber meets both of these requirements. Optical attenuation in fact ranges between 0.2 and 2.0 dB/km while the modulation bandwidth is inherently almost infinite in single-mode fibers for most telecommunication applications. In general, it is not possible to specify just one number to characterize either the attenuation or the modulation bandwidth of optical fiber because both parameters are strongly influenced by the operating wavelength and optical waveguide structure. For example, in the limiting case of single-mode optical fiber linearly excited by a highly coherent externally modulated laser source the link bandwidth is limited only by the modulating signal bandwidth and by fiber polarization mode dispersion. Under these conditions, ITU-T STM16 transmission at 2488 and 320 Mb/s can reach more than 1000 km at 1550 nm without being particularly limited by pulse dispersion of the bandwidth limitation. However, even the extremely low attenuation of less then 0.2 dB/km available at 1550 nm would require a link budget of 200 dB in order to be connected. This extremely high attenuation can be overcome by using optical amplifiers with a repetition span of about 25 dB between each of them.

The picture is completely different when using multimode optical fibers. Before entering into more detail, it is useful first to describe the waveguide properties of optical fibers. The optical fiber is a cylindrical dielectric waveguide where the guiding principle is achieved using the refractive index difference between the inner dielectric region, the core and the outside dielectric region, the cladding. Making the refractive index slightly higher in the core than in the cladding ensures optical waveguide operation in a specific wavelength range.

The optical fiber dealt with here is made of a silica glass composition and both the core and the cladding must be carefully doped and processed in order to obtain the exact refractive index profile and high-purity material needed to achieve simultaneously very low dispersion and attenuation. The low attenuation wavelength range is achieved by choosing the correct silica glass to place the dielectric optical waveguide structure within the near-infrared region, $820 \, \text{nm} < \lambda < 1620 \, \text{nm}$. In this wavelength range, the optical fiber will perform in the single-mode or multimode regimes depending on the radius a of the inner core region. Standard single-mode fibers have the core diameter close to $a = 4 \, \mu\text{m}$ or less, while standard multimode fibers have a much larger core radius, either $a = 25 \, \mu\text{m}$ or $a = 31.25 \, \mu\text{m}$. Other factors affect the modal capability of the fiber, but essentially the core diameter is mainly responsible for the different kinds of waveguide behavior. Figure 1.1 shows a schematic drawing of the multimode fiber geometry.

This book will deal exclusively with multimode fibers, so cylindrical dielectric waveguides made of doped silica glass with a core diameter of either $50 \, \mu\text{m}$ or $62.5 \, \mu\text{m}$ will be referred to implicitly. These multimode fibers are specified by ISO/IEC 11801 and ITU-T G.651 standards. The multimode regime requires a strong bandwidth limitation compared to single-mode ones. This is essentially because of the multipath propagation and the related group delay per unit length spreading among
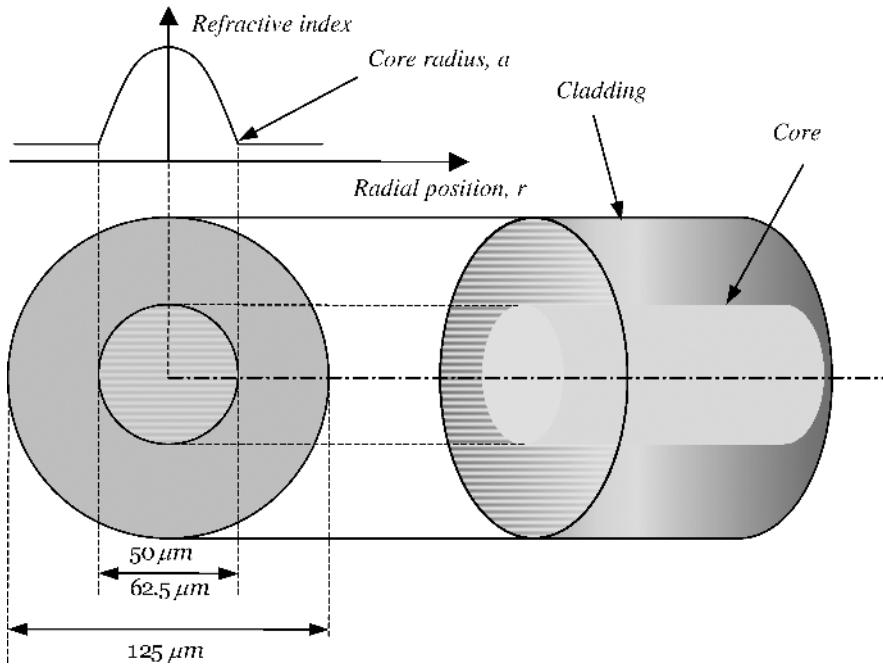
Figure 1.1 Multimode fiber geometry

all allowed and excited modes. The refractive index profile is the only functional parameter that sets the electromagnetic properties of every dielectric waveguide. In order to compensate for different mode delays it is possible to design a graded refractive index profile. Accordingly, the mode delay per unit length is equalized and in principle the modal bandwidth would be infinitely large for perfectly compensated delays. In reality, group delay compensation is an extremely critical function of the refractive index profile and even assuming a highly sophisticate manufacturing process the highest modal bandwidth achieved for commercially available optical fiber usually does not exceed a few gigahertz per kilometer. In addition to modal dispersion, each mode is subjected to intrinsic chromatic dispersion due to the dispersion relationship between the modal propagation constant and the source spectrum width. Chromatic dispersion is otherwise identified as group velocity dispersion (GVD) and is the major drawback in dispersion-limited transmission using single-mode fiber with direct modulated semiconductor laser diode sources.

Every nonlinear behavior and dispersion contribution to pulse propagation experienced by single-mode fiber transmission would in principle be present even for each individual mode of every multimode fiber. Of course, the very different timescales of these phenomena with respect to modal dispersion makes the contribution of almost all of them negligible when considering pulse dispersion in multimode fibers. Accordingly, in the following chapters the theory of the multimode pulse response will be presented, including only modal and chromatic dispersion.

1.3 Semiconductor Laser Sources

There is a need to increase the transmission bit rate for high-speed laser sources, due to well-performing and low-cost direct modulation capabilities of those devices compared with the slow

and much less efficient LED. Recently, VCSEL technology provides a very interesting compromise in terms of speed, cost, yields and power consumption. However, more consolidated light sources for 10GbE, at least in the 1310 nm wavelength range, are still directly modulated Fabry-Perot (FP) lasers and distributed feedback (DFB) lasers. Unfortunately, any kind of laser source is almost a nightmare for every multimode fiber.

There are at least three characteristics of semiconductor lasers that act against the natural behavior of any multimode optical waveguide and of the multimode fiber in particular:

1. The light emitted from the semiconductor laser is spatially localized on to a region that is usually much narrower then the fiber core area. This leads to a partial excitation of a few mode groups allowed by the fiber. If the group delay of the multimode fiber is not compensated enough among excited bound modes (the amount of compensation required depends on the ratio between the bit rate and the differential mode delay), the energy distribution among a few excited modes will result in a consistent pulse broadening at the fiber end facet after just a few hundred meters of propagation length.
2. The laser coherence properties in conjunction with multimode connectors originate in the intensity-dependent Speckle noise term, namely the modal noise.
3. The power distribution among fiber modes is strongly dependent on the combined effect of launch polarization and environmental induced stresses and perturbation, originating in random output pulse fluctuations, which of course make the channel picture even more complicated.

A large number of measurements demonstrates how unpredictable the MMF frequency response would be when the light excitation comes from a laser source. The reason for such unpredictable behavior results from the very spatially localized excitation of a subset of guided modes in the MMF. Depending on which fiber modes are excited by the laser light, either a very high or a very low propagation bandwidth can be experienced on the same MMF link. When the light power is distributed among a few supporting modes, even a small propagation delay difference among excited modes will make a strong output pulse deformation with the creation of relatively large pulse precursors and postcursors that destroy pulse symmetry.

The launching-dependent frequency response of every multimode optical fiber clearly complicates the picture of multigigabit transmission over this dielectric waveguide. The IEEE802.3ae standard for 1GbE specifies the restricted offset launch conditions as the solution to provide suitable fiber mode excitation in order to control differential mode delay and pulse broadening. Even if restricted offset launch conditions provide a more stable multimode fiber bandwidth behavior, their implementation is not so simple as to be widely accepted and leads to increasing cost per module and other practical implications.

1.4 Offset Launch Conditions

A standard solution proposed to improve the multimode fiber bandwidth by limiting multipath propagation relies on specified offset launch conditions and related encircled flux specifications using standard offset launching patchcord. The idea behind offset launching is to excite selectively high-order modes that are localized in the mid-region of the fiber core section. Figure 1.2 shows qualitatively the offset launch case.

Unfortunately, offset launch patchcord is almost impractical today because of its dimensions and the space required to be hosted into small modules or crowded boards, as well as the cost issue. Sometimes, the cost of offset launching patchcord is comparable to the cost of the whole module. In addition, a unique solution for defining offset launch compliant with both 50 µm and 62.5 µm multimode fibers is still under study.
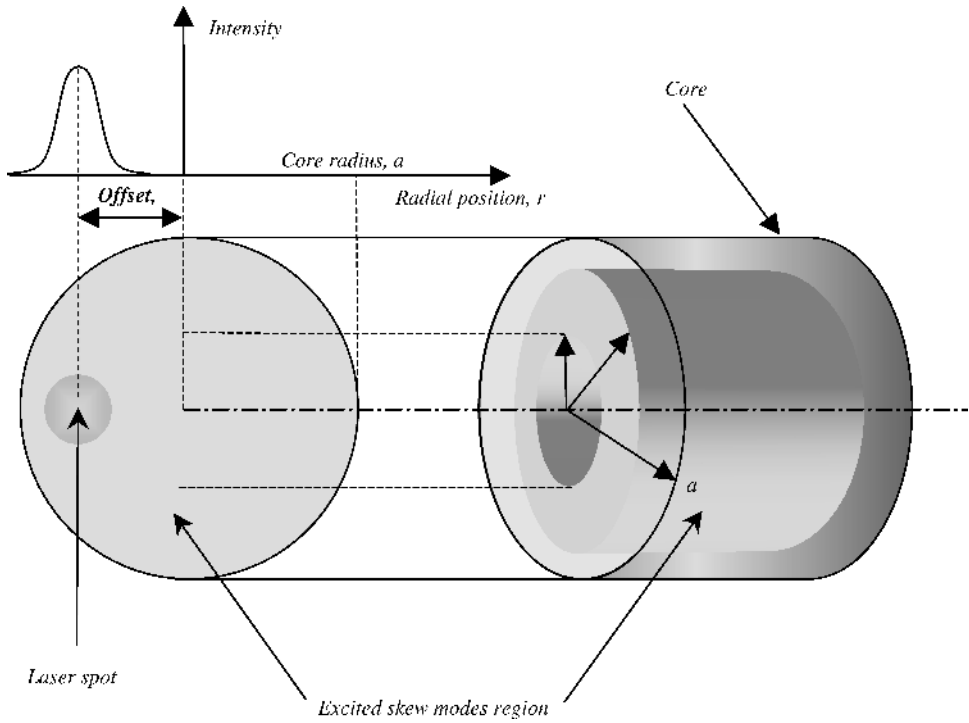
Figure 1.2 Schematic representation of the offset launch in a multimode fiber. The offset coordinate is ρ. Excited skew modes occupy the inner shaded region around the radial position ρ, leaving both the central region and the outer core region almost unoccupied by the electromagnetic energy

1.5 Optical Receivers

The optical receiver converts the optical signal available at the fiber end section into the corresponding electrical signal. This process takes place inside the optical photodetector according to the photoelectric effect. Each incoming photon has a probability of being absorbed, releasing its energy to a conduction band electron. The probability of photodetection depends on several factors involving the detector optical coupling, antireflection coating, depth of the intrinsic absorbing region, leakage currents and so on. All of these factors are usually summarized using a single parameter, namely the photodetector external quantum efficiency, $\eta_p(\lambda)$. Typical values range between $50\% < \eta_p(\lambda) < 95\%$, depending on the operating wavelength and photodetector structure. Very high-speed photodiodes have among the lowest quantum efficiency values due to width shortening of the absorbing region, thus minimizing the transit time dispersion. Coaxial receptacle photodiodes, designed for 10GbE applications in the second window operations $\lambda = 1310$ nm, usually have quantum efficiency in the order of $60\% < \eta_p(\lambda) < 80\%$.

Each photon brings a fixed energy amount depending on its wavelength. The detected photon rate, namely the number of photons per unit time incident on the photodetector sensible area, is therefore related to the received optical power. The conversion factor is the universal constant R_0:

$$R_0 = \frac{q\lambda}{hc} \quad \text{(A/W)} \tag{1.1}$$

Substituting the speed of light in a vacuum, $c = 2.9979 \times 10^8$ m/s, and the electron charge, $q = 1.6022 \times 10^{-19}$ C, for the Plank constant, $h = 6.626110^{-34}$ J s, the following value for the conversion factor as a function of the wavelength is obtained:

$$R_0 = 0.8066\lambda_{[\mu m]} \Rightarrow \begin{cases} \lambda = 0.850 \,\mu m \rightarrow R_0 = 0.686 \text{ A/W} \\ \lambda = 1.310 \,\mu m \rightarrow R_0 = 1.057 \text{ A/W} \\ \lambda = 1.550 \,\mu m \rightarrow R_0 = 1.250 \text{ A/W} \end{cases} \qquad (1.2)$$

The product of the conversion factor $R_0(\lambda)$ with the photodetection external quantum efficiency $\eta_p(\lambda)$ defines the photodetector responsivity $R(\lambda)$:

$$R(\lambda) = R_0(\lambda)\eta_p(\lambda) = \frac{q\lambda}{hc}\eta_p(\lambda) \quad \text{(A/W)} \qquad (1.3)$$

Assuming that the photodetection external quantum efficiency $\eta_p(\lambda) = 0.7$ is independent of the operating wavelength, from Equation (1.2) the following expected values of photodiode responsivity for 10GbE applications are obtained:

$$\eta_p = 0.7 \Rightarrow \begin{cases} \lambda = 0.850 \,\mu m \rightarrow R_0 = 0.480 \text{ A/W} \\ \lambda = 1.310 \,\mu m \rightarrow R_0 = 0.740 \text{ A/W} \\ \lambda = 1.550 \,\mu m \rightarrow R_0 = 0.875 \text{ A/W} \end{cases} \qquad (1.4)$$

It should be noted, however, that the photodetection external quantum efficiency is a decreasing function of the wavelength. This effect compensates partly for the linear reduction of the conversion constant in Equation (1.2) at shorter wavelengths.

The photocurrent is proportional to the envelope of the received optical intensity, and for this behavior the photodiode is defined as a square-law device. The optical power is then converted into electrical current intensity, as clearly reported by the unit of measure of the responsivity function in Equation (1.3). At a limited input optical power level, the photodiode behaves linearly with respect to the incident optical intensity and can be conveniently characterized by the impulse response and the transfer function in the frequency domain. The photodetector therefore performs the first filtering process on the incoming optical signal. The photocurrent pulses are then amplified and converted into more suitable voltage pulses before being processed through conventional clock and data recovery (CDR) circuits. If the multimode fiber bandwidth together with additional electrical low-pass filtering in the optical receiver front end set severe limitations on the signal available at the receiver decision section, a large error rate would be expected and a transmission failure status would therefore be detected. This failure mechanism is referred to as the 'dispersion limited system fault'. The only possible remedies known to overcome this fault condition is either to provide a received pulse reshaping process or to use error correcting code transmission or even reduce the signal bandwidth requirement in the given transmission channel using a proper modulation format. The first approach leads to the electronic dispersion compensation (EDC) technique, while two other solutions, optical mode filtering (OMF) and the multilevel modulation format (PAM-4), tend to either increase the multimode fiber transmission capacity or reduce the signal bandwidth occupation.

1.6 Signal Compensation Techniques

Due to the relatively large differential mode delay (DMD) encountered in multimode fibers when excited by semiconductor laser sources, a strong pulse dispersion and interferometric noise (Speckle pattern) are simultaneously expected as major limitations to multigigabit data transmission over a few hundred meters of link length. These effects lead to different dispersion compensation approaches, namely electronic dispersion compensation (EDC), optical mode filtering (OMF) and

quaternary pulse amplitude modulation (PAM-4). The IEEE 802.3aq 10BASE-LRM Committee is at present carefully investigating these three alternative compensating procedures.

The impulse response of a multimode fiber link distributed over several connected sections is very sensitive to perturbing environmental conditions like temperature mechanical vibration and even the state of polarization. Due to its inherent adaptive architecture, EDC seems to have better control against those environmental effects, making the multimode fiber link more robust under cabled operating conditions. However, it is widely accepted by the IEEE 802.3aq Committee that the complete picture of 10GbE over long-reach multimode fibers remains quite troublesome unless a proper dispersion compensation mechanism is taken into account. Although EDC seems to be the most promising solution for multipath pulse dispersion compensation, the remaining two approaches are still under investigation and merit some attention as alternative methods for potential future approaches. In the following, the operating principles of the above-mentioned three methods will be considered. All of the considered solutions have several issues to be solved in order to become widely deployed on the 10GbE large-volume market expected in 2006 and 2007. The basic principles of these signal compensation techniques for multigigabit transmission over multimode optical fibers will also be reviewed.

1.6.1 Electronic Dispersion Compensation (EDC)

The electronic dispersion compensation (EDC) technique proposes to mitigate optical pulse broadening at the multimode fiber output by means of electronic signal processing directly operating at the signal rate. The optical signal must be first detected and linearly amplified by a proper low-noise receiver before being processed by EDC. This approach requires relatively complex digital signal processing at 10 Gb/s in the case of the 10BASE-LRM standard. The key element is the adaptive finite impulse response (FIR) filter whose tap coefficients are managed through the minimum mean square error (MMSE) algorithm. Among several different available architectures the most suitable for achieving simultaneously a high bit rate capability and relatively low power requirements is based on a combination of the *feedforward equalizer* (FFE) and the *decision feedback equalizer* (DFE). Both sections are realized by means of FIR filters. Key parameters of both the FFE and DFE are the number of taps and the tap delay (tap spacing) used to synthesize each FIR filter. The more dispersed equalizer is expected to be the input pulse and the longer are would be the filter length in order to compensate for longer precursors and postcursors. This produces a trade-off between technological complexity, power consumption and compensation capability. Essentially, the EDC action can be depicted in two steps:

1. The FFE section controls the input pulse shape providing weighted amounts of frequency response equalization in order to re-establish a proper pulse profile, thus reducing the intersymbol interference pattern.
2. The DFE section adaptively adjusts the decision threshold of the digital quantizer in order to minimize the intersymbol interference power at the decision section output. According to standard solutions, the DFE operation requires the clock recovery feature from the incoming data pattern in order to synchronize the decision timing properly.

In this context, relatively relaxed optical constraints including launch conditions, connector tolerances and optical detection architectures are required for the fiber transmission system. The EDC advantage relies on its integrated circuit (IC) structure: low cost, high reliability, compact and easily integrable in a small form factor and pluggable data communication modules. The EDC drawback is that some unstable convergence is experienced when the required filter length increases and the multimode fiber response demands that the compensation capabilities be limited. A low value of the signal-to-noise ratio (SNR) at the optical receiver input places one more constraint on EDC

operation. The electronic compensator architecture should also include an adaptive electrical filter in order to track the compensation profile variations according to the temporal changes of the MMF response and to restore the proper electrical pulse profile at the decision section.

It will be seen in the next chapters that several fiber modes excited by the laser source will propagate, with relative delay differences giving rise to multipath pulse distortion after some distance from the launch section. Due to the large-area photodetection mechanism, interferometric noise plays a marginal role, leaving the complete interferometric pattern inside the detected light area. Spatial averaging over the whole fiber end section due to the large-area detection mechanism makes the detected light intensity spatially averaged and almost unaffected by interferometric noise fluctuations.

Major problems in the EDC approach are:

1. The efficiency of the FFE filter depends on the number of taps and on the relative spacing needed for impulse reconstruction. Due to the strong multipath dispersion usually encountered in legacy multimode fibers, several integral bit time equivalents are needed, leading to long FFE filter structures with more than 9 to 12 sections.
2. Increasing the number of taps leads to an increase in the equalization filter capability of the long pulse tail distortion, but at same time it increases considerably the power consumption and the design implementation complexity for the given technology state.
3. Internal delay of the EDC architecture must match with 10GbE bit-rate requirements (about 100 ps time step) and this leads to state-of-the-art CMOS (complementary metal oxide semiconductor) technology with less than a 90 nm gate length
4. The input stage must account for a linear automatic gain controlled (AGC) microwave amplifier with a proper dynamic range and a smooth bandwidth in excess of 8 GHz.
5. The optical photodetector and related low noise transimpedance amplifier must have a linear (V/W) transfer characteristic.
6. The DFE corrects only the pulse postcursor. Inherent leaking of the compensation capability of either pulse precursor and the dual peak pulse response reveal a severe limitation of the DFE approach for these pulse distortions.

1.6.2 Optical Mode Filtering (OMF)

The optical mode filtering (OMF) technique proposes a reduction in the number of propagating modes in the multimode fiber by selective excitation and detection of the fundamental fiber mode. Optical mode filtering can be summarized using the following basic operations:

1. A selective laser light launch into the multimode fiber input section in order to couple as much power as possible to the fundamental fiber mode only. This is achieved by means of a proper laser coupling mechanism in order to maximize the overlapping integral with the fundamental fiber mode.
2. Selective light detection at the multimode fiber end section by means of a spatial selective filter interposed between the multimode fiber end section and the photodetector active area.

By reducing drastically the number of excited mode groups, modal delay spreading is implicitly reduced. The principal problem encountered by this method is the large amount of power fluctuation (modal noise) induced by the standard connector offset and perturbing environmental conditions. However, under controlled laboratory conditions, this solution provided excellent results. From an application point of view, this solution requires specialized launch and detection tools that add complexity and cost to high-volume market demands. It is a common opinion of the IEEE 802.3aq

Committee that in order to introduce OMF as a valid signal compensation technique it should work together with EDC. Of course, the performance required in this case by EDC would be much less demanding than in a stand-alone application, but would still add more complexity and cost to the module final solution.

As had been anticipated, the basic principle behind OMF is to force as much multimode fiber as possible to operate as nearly single-mode fiber in the 1310 nm region by selective excitation and selective detection of the fundamental fiber mode. In the OMF approach, only the fundamental fiber mode would be excited in principle, leaving a relatively small contribution in terms of pulse energy carried up to the fiber end to the residually excited higher-order modes. In other words, the basic idea behind OMF is to force a single-mode regime into a multimode fiber. Although in principle the differential mode delay and the modal bandwidth concepts no longer apply to the OMF approach, the interferometric noise between excited higher-order modes and the fundamental mode grown at each fiber discontinuity, like connectors and fusion splices, makes the whole channel design much more critical with respect to optical alignment tolerances when compared to the EDC approach. Every misalignment in the fiber core contributes to unwanted higher-order mode excitation and modal noise. An additional effect is represented by the polarization of the fundamental mode respect to the direction connector misalignment. Due to the random nature of the polarization direction of the fundamental mode and to its sensitivity to any environmental condition, a polarization-dependent noise term must be added to light intensity. A careful central spot size launching condition, receiver mode filtering and optical connector alignment statistics all play a dominant role in the OMF approach. Unfortunately, standard tolerances for MMF technology optical connectors are too loose to compete with the OMF requirements. High modal noise due to an interference pattern between higher order modes and the fundamental mode severely limits system performance.

Major problems in the OMF approach are:

1. The laser source coupled field must match the fundamental fiber mode in order to transfer as much power as possible to that mode. This in particular requires numerical aperture adaptation between the laser light and the fundamental fiber mode.
2. Due to almost unavoidable irregularity of the refractive index profile at the fiber center (dip or pin) laser light should not be focused on such a small area around the fiber axis. Laser light should be applied to a larger axial-symmetric region in order to minimize the relative power coupled in the defective central region, but a region not too large to provide unwanted higher mode excitation.
3. Minimize the power transferred to higher-order modes.
4. Connector offset plays a dominant role in OMF penalty calculation. Any offset leads to power coupling that is not optimized, allowing higher-order mode excitation and consequent pulse dispersion.
5. Polarization and connector offset generate relevant modal noise.
6. The modal filter at the receiver end is needed to cut out higher-order mode contributions to the detected intensity, but it generates strong intensity fluctuations when modal noise, polarization and connector offset are produced simultaneously.

1.6.3 Quaternary Pulse Amplitude Modulation (PAM-4)

The basic idea behind the quaternary pulse amplitude modulation (PAM-4) proposal is to reduce the bandwidth requirement of the multimode fiber link in order to allow full 10GbE datastream transmission over a long-reach legacy multimode fiber link. This is achieved by using four-level modulation amplitude instead of the more conventional two-level NRZ (no return to zero) modulation scheme. Adopting the four-level scheme, each sequence of two information bits is coded

into the four-level digital amplitude instead of being simply time multiplexed, as shown by the following encoding logic:

$$
\begin{bmatrix}
b_1 & b_2 & L & I_2 + I_1 & I_{\text{mod}} \\
\hline
0 & 0 & L_0 & 0+0 & 0 \\
0 & 1 & L_1 & 0+I & I \\
1 & 0 & L_2 & 2I+0 & 2I \\
1 & 1 & L_3 & 2I+I & 3I
\end{bmatrix}
$$

This shows the encoding relations between the NRZ dual-bit sequence (b_1, b_2) and the logic PAM-4 levels L_k, $k = 0, 1, 2, 3$. Each PAM-4 logic level is then identified by combining the two current generators I_1 and I_2. The corresponding modulation current I_{mod}, reported in the last column, is injected into the laser.

The result is that for the same symbol rate exactly half a bit rate is required. Referring to the 10GbE signaling speed $B = 10.3125$ Gb/s, this translates into one-half of the symbol rate requirement, corresponding to exactly $B_{\text{PAM-4}} = \frac{1}{2}B = 5.15625$ Gb/s. Assuming that the multimode fiber modal bandwidth scales inversely with the link length (no mode group mixing), this leads to double the link length or one-half of the link bandwidth requirement for the fixed link length. Since there is interest in transmitting 10GbE, the latter conclusion looks quite attractive, allowing in principle 10GbE transmission over at least 300 m of legacy multimode fiber with a modal bandwidth $\widehat{BW}$ (bandwidth per kilometer) $= 500$ MHz km in the second window region.

Although the conclusion above could justify design efforts in the PAM-4 solution due to sensible relaxation of multimode fiber bandwidth requirements, major constraints will be added to the optoelectronic modules.

1.6.3.1 NRZ to PAM-4 Encoder

Figure 1.3 shows a solution for the PAM-4 encoder operating in the optical domain. The current encoding logic is represented by the following relationships:

$$
\begin{cases}
I_{\text{mod}} = I_1 + I_2 \\
I_L = I_{\text{mod}} + I_{\text{bias}}
\end{cases}, \qquad
\begin{cases}
I_1 = \begin{pmatrix} I : \text{high} \\ 0 : \text{low} \end{pmatrix} \\
I_2 = \begin{pmatrix} 2I : \text{high} \\ 0 : \text{low} \end{pmatrix}
\end{cases}
\tag{1.5}
$$

The laser diode driver LDD_1 delivers the modulation current I_1 that assumes two digital levels, namely $I_1 = I$ and $I_1 = 0$ in the high state and in the low state respectively. The laser diode driver LDD_2 delivers the modulation current I_2 that still assumes still two digital levels, but of double intensity, namely $I_2 = 2I$ and $I_2 = 0$ in the high state and in the low state respectively. According to the 1:2 demultiplexed function, each laser driver is fed at half the bit rate and each of them supplies the proper output current corresponding to the input digital level. Depending on the input dual-bit sequence, four input combinations are possible and correspondingly four output current levels are coded. Due to the 1:2 demultiplexed function, each output current level is associated with twice the input time step $T = 1/B$, effectively doubling the duration of each PAM-4 coded symbol.

The most relevant problem concerning the optical transmitter for the PAM-4 coding is the linearity of the laser characteristic and the resulting signal-to-noise ratio uniformity achievable for each level difference. It is well known that the laser pulse response is strongly dependent on the biasing position, at least when the laser is biased close to the lasing threshold. Different overshoot and transient time responses are therefore expected for the level transitions $L_0 \rightarrow L_1$ and $L_2 \rightarrow L_3$, due to the different positions of L_0 and L_2 respectively compared to the lasing threshold.
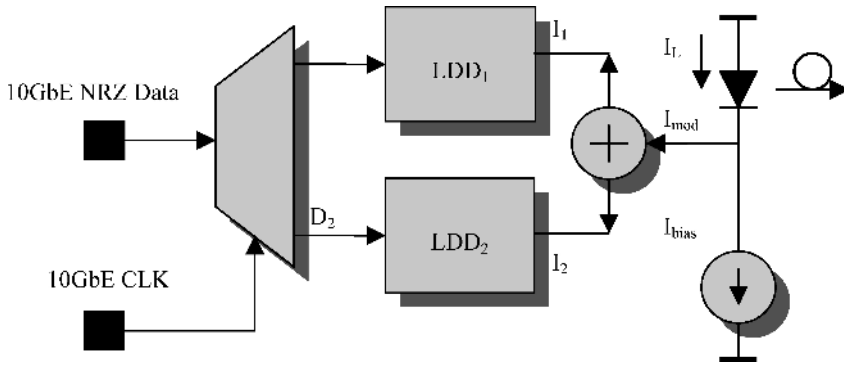
Figure 1.3 Block diagram of the NRZ to PAM-4 optical encoder. The modulation current is given by the sum of the two current components I_1 and I_2

In order to understand the signal differences better, Figure 1.4 illustrates both the NRZ signal and the corresponding PAM-4 converted signal. The first row in Figure 1.4 shows the incoming NRZ pattern. The following two waveforms represent the 1:2 demultiplexed signals with ideal timing. In order to align those waveforms it is necessary to add a time delay equal to one time step T to waveform D_1. The resulting shifted signal is then represented. The current sum shown in the schematic in Figure 1.3 therefore provides the PAM-4 output reported. This is the modulation current pattern that drives the semiconductor laser.

1.6.3.2 PAM-4 to NRZ Decoder

Once the optical PAM-4 signal reaches the photodetector it must be recognized and converted to NRZ using a proper PAM-4 to NRZ decoder. Figure 1.5 gives the block diagram for a plausible solution for the PAM-4 to NRZ decoder.

The basic principle underlying the schematic PAM-4 to NRZ decoder presented in Figure 1.5 considers the three inner level transitions of the PAM-4 signal to be three separate NRZ signals of reduced amplitude. After detection, the logic block recovers the original NRZ pattern. The major constraint in the PAM-4 to NRZ decoder is the reduced signal-to-noise ratio available at each threshold detector in the optical receiving process in comparison to the equivalent NRZ optical receiver. It is important to underline the fact that the comparison between NRZ and PAM-4 optical receivers should be performed using adequate assumptions and available technology.

1.6.3.3 NRZ versus PAM-4: SNR Comparison

In order to calculate the signal-to-noise ratio and proceed to evaluate the different benefits and impairments between NRZ and PAM-4 modulation schemes, consider the following assumptions:

1. NRZ and PAM-4 optical receivers use the same IC technology with the same white thermal noise power spectral density n_{th}. This allows only noise bandwidth differences to be considered as responsible for the different noise powers available in the two receivers.
2. Both optical receivers are thermal noise limited. In other words, thermal noise is the dominant contribution in setting the sensitivity performances.
3. NRZ and PAM-4 optical receivers both have the same frequency response profile, but the NRZ receiver has twice the bandwidth of the PAM-4 receiver.

NRZ
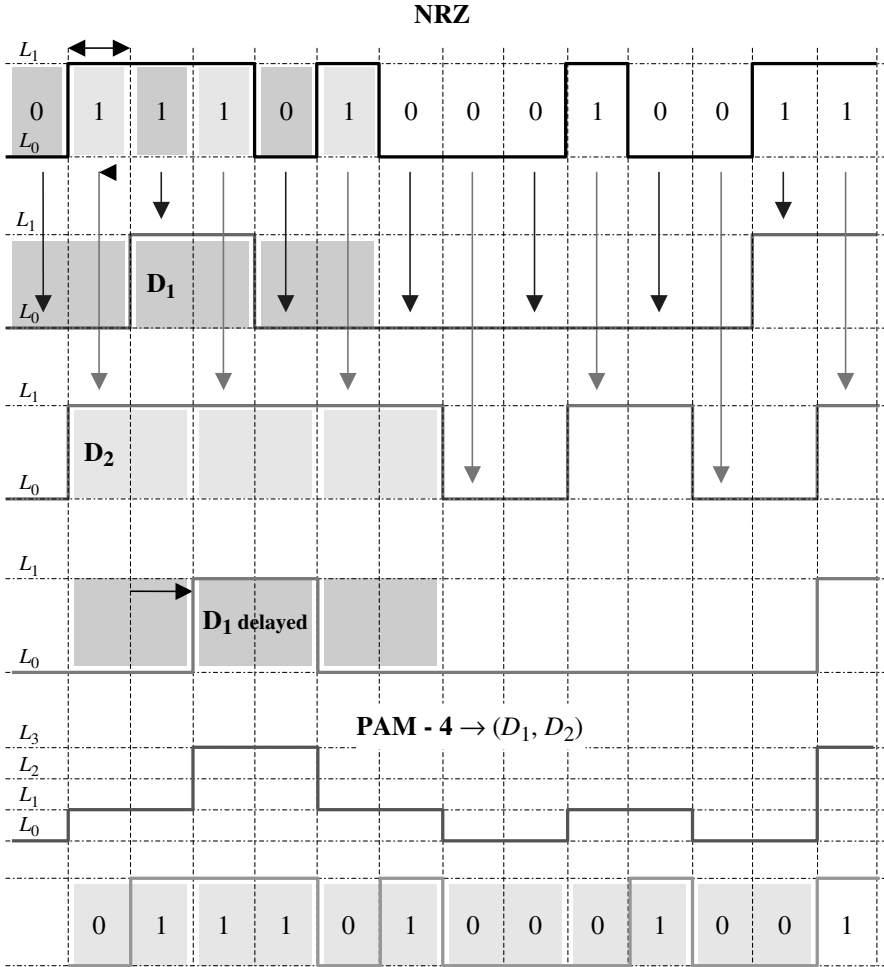
Figure 1.4 NRZ to PAM-4 signal encoding according to the block diagram presented in Figure 1.3. Light waveforms are detected at the 1:2 demultiplexed output including T-delay required in order to align signal wavefronts before the current sum. The waveform shows the total modulation current injected into the laser according to the coded PAM-4 pattern

Figure 1.6 is a schematic representation of the frequency response and related noise bandwidth of both receivers. According to the third assumption, the two receivers have a noise bandwidth ratio equal to their corresponding bandwidths. Therefore:

$$B_{\mathrm{n,NRZ}} = 2B_{\mathrm{n,PAM\text{-}4}} \tag{1.6}$$

From assumptions 1 and 2, it can easily be deduced that the noise power of the NRZ receiver is twice the noise power of the PAM-4 receiver:

$$\sigma_{\mathrm{n,NRZ}}^2 = B_{\mathrm{n,NRZ}}n_{\mathrm{th}} = 2B_{\mathrm{n,PAM\text{-}4}}n_{\mathrm{th}} = 2\sigma_{\mathrm{n,PAM\text{-}4}}^2 \tag{1.7}$$
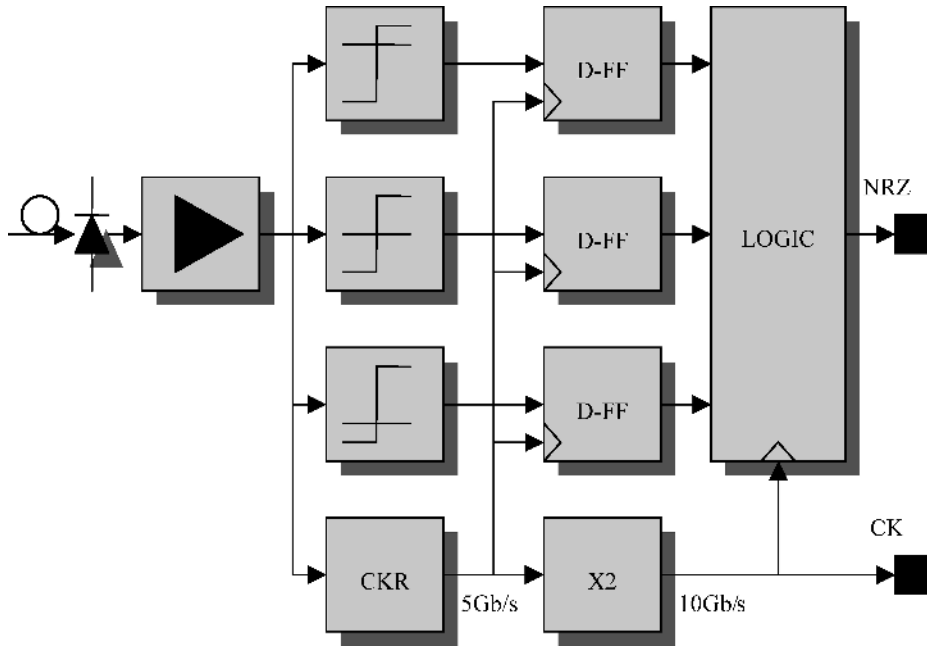
Figure 1.5 Schematic representation of the block diagram of a PAM-4 to NRZ decoder using three threshold detectors and a clock by 2 multiplier. By choosing the correct threshold position of the three threshold detectors, the subsequent logic can reconstruct the original NRZ signal from the PAM-4 detected signal
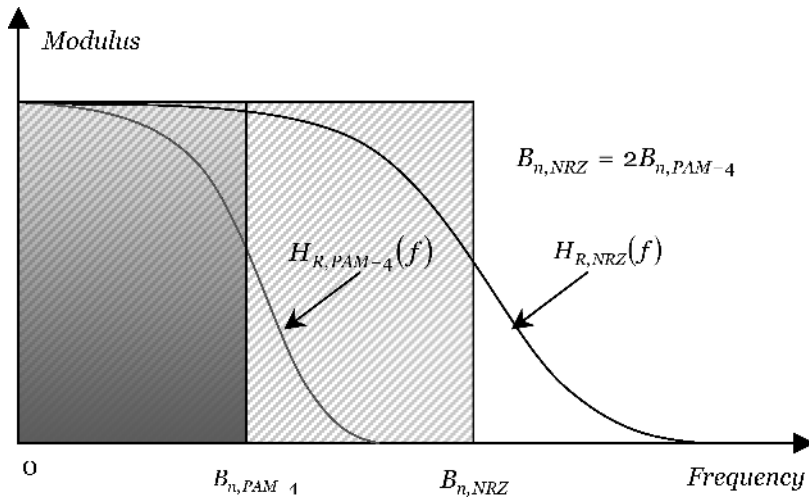
Figure 1.6 Schematic representation of frequency responses and noise bandwidths of NRZ and PAM-4 receivers. According to the third assumption, noise bandwidths have the same ratio of $\frac{1}{2}$ as their respective cut-off frequencies

The RMS (root mean square) noise reduction Δ_n produced using the PAM-4 receiver can be estimated as

$$\Delta_n \equiv 10 \log_{10} \left(\frac{\sigma_{n,NRZ}}{\sigma_{n,PAM-4}} \right) = 10 \log_{10} \sqrt{2} \cong 1.5 \text{ dB(optical)} \tag{1.8}$$

The gain factor Δ_n represents the average optical power sensitivity improvement for achieving the same signal-to-noise ratio performances for a given signal amplitude. If the required decision threshold distance had been the same for both NRZ and PAM-4 receivers, it can be concluded that there is a net gain of 1.5 dB (optical) when using the PAM-4 solution versus the NRZ one, but unfortunately this is not the case. In fact, for a given average received optical power P_R, the PAM-4 signal has a one-third decision amplitude with respect to the corresponding NRZ signal. The signal pattern reported in Figure 1.4 gives a qualitative representation of this characteristic behavior. Figure 1.7 shows the computed gain between the PAM-4 and the NRZ line coding versus increasing multimode fiber link length for a specified modal bandwidth of $\widehat{BW} = 500$ MHz km with Gaussian frequency response. Figures 1.8 and 1.9 show instead a more realistic computer simulation of both NRZ and PAM-4 eye diagrams, assuming that they have the same average optical power for the 10GbE case. The pulse has been chosen according to the raised cosine family with unit roll-off.

Since there is no intersymbol interference (ISI) in both cases, the reduction in the decision amplitude experienced for each signal transition in the PAM-4 pattern with respect to the NRZ one
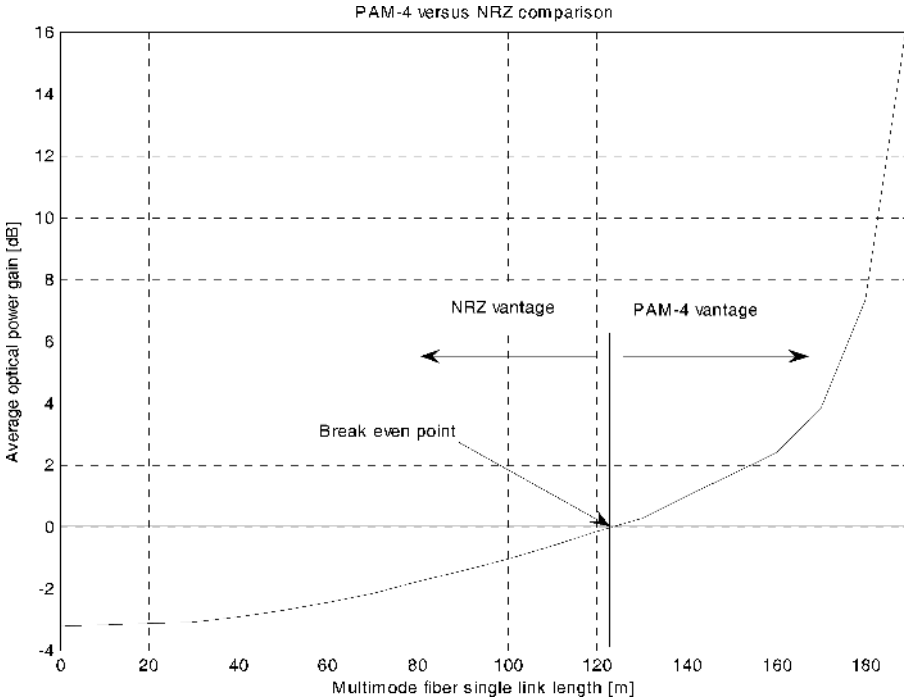
Figure 1.7 Optical sensitivity gain comparison between the PAM-4 and NRZ line codings versus the multimode fiber single link length. The fiber modal bandwidth is $\widehat{BW} = 500$ MHz km. The breakeven distance is about $L_0 = 123$ m

PPG PARAMETERS
Line code: NRZ
Pulse: Raised-Cosine

Roll-off = 1
HWHM = 5.1563GHz
Bit-rate = 10.3125Gb/s

PPG OUTPUT
Single Pulse: Raised-Cosine Time Response

Single Pulse: Raised-Cosine Spectrum - Magnitude

Eye Diagram: PRBS 2⁷-1

Single Pulse: Raised-Cosine Spectrum - Phase
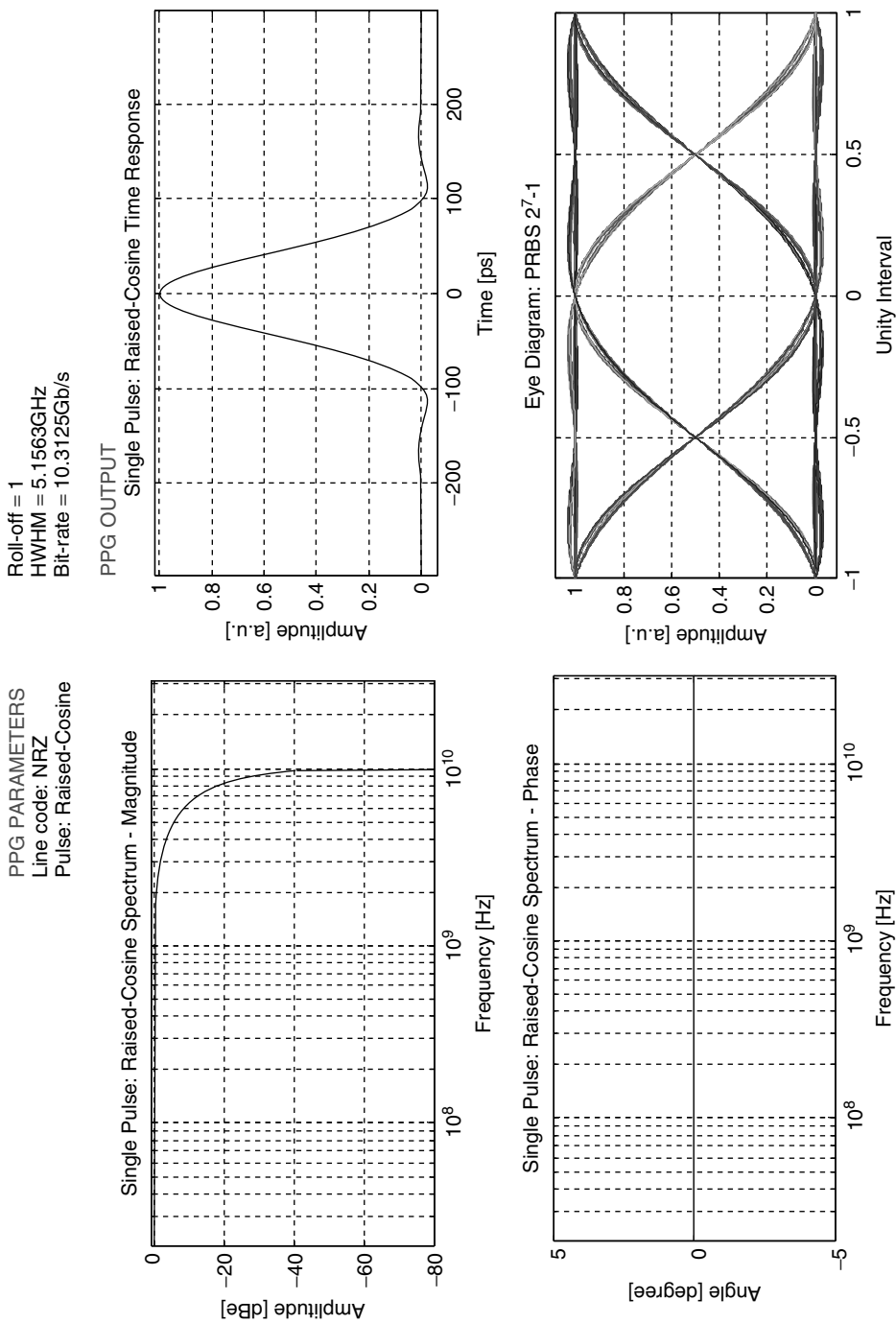
Figure 1.8 Frequency and time domain representations of NRZ PRBS 2^7-1 line code signals at 10GbE data rate. Left top represents the single pulse according to the unity roll-off raised cosine profile, while the left bottom graph shows the corresponding eye diagram in normalized bit time units

Figure 1.9 Frequency and time domain representations of PAM-4 PRBS 2^7-1 line code signals at 10GbE data rate. Left top represents the single pulse according to the unity roll-off raised cosine profile, while the left bottom graph shows the corresponding eye diagram in normalized bit time units. A scaling factor of 2 has been introduced in the raised cosine pulse profile with respect to the NRZ case shown above

leads to a loss of signal strength of about 4.77 dB (optical):

$$\Delta_s = 10\log_{10}(1/3) \cong -4.77\,\text{dB} \tag{1.9}$$

This value refers to ideal eye diagrams with no added jitter or ISI and the average eye opening coincides with the decision threshold amplitude for each level. The receiver sensitivity for a given bit error rate (BER) is determined by the Q-factor defined below, where d is the decision threshold distance and σ is the total RMS noise amplitude. Assuming thermal noise limited detection and Gaussian noise approximation, then

$$Q \equiv \frac{d}{\sigma}, \qquad \text{BER} = \frac{1}{2}\text{erfc}\left(\frac{Q}{\sqrt{2}}\right) \tag{1.10}$$

Taking into account the reduced noise bandwidth in Equation (1.8) for PAM-4 and the corresponding detection amplitude reduction in Equation (1.9), it can be concluded that the net average optical power gain using the PAM-4 receiver instead of the corresponding NRZ receiver is about 3.27 dB (optical):

$$\Delta_Q = \Delta_s + \Delta_n \cong -4.77 + 1.50 = -3.27\,\text{dB} \tag{1.11}$$

This is essentially the reason for the success of the NRZ solution adopted in almost all optical telecommunication systems. Of course, at least technically the development of the PAM-4 signaling must be justified.

1.6.3.4 NRZ versus PAM-4: Eye Opening Comparison

The general signal-to-noise reduction experienced by the PAM-4 signal must in fact be balanced by the reduced channel bandwidth requirement, as clearly shown by comparing the left top graphs of Figures 1.8 and 1.9. Assuming the same unity roll-off raised cosine signal pulse profile in both modulation codes, it is evident that the PAM-4 pulse requires exactly a bandwidth that is one-half of the corresponding NRZ case. This leads to a considerable pulse spreading reduction after a given link length propagation, which corresponds to a relative increased optical eye opening. Following this reasoning, it is possible to arrive at the obvious conclusion justifying the PAM-4 coding when reduced transmission channel capabilities must be accounted for in the transmission system design.

Figures 1.10 and 1.11 report respectively the PAM-4 and NRZ data stream detected after a single link length of 100 m of a Gaussian bandwidth multimode fiber. Most of the original eye opening reduction due to multilevel coding has been recovered after just 100 m of link length. In fact, the PAM-4 eye opening diagram results from about 27 % of the highest PAM-4 signal amplitude, while the same qualitative calculation performed on the NRZ eye diagram shows that the eye opening results from about 50 %. Referring to the ideal -4.77 dB penalty reported in Equation (1.9), the ratio now gives about -2.67 dB, with a recovery of about 2.1 dB. Assuming the same noise spectral power density for both line codes, the net gain in using PAM-4 versus NRZ is still negative, -1.17 dB, but is much more reduced compared to the back-to-back case in Equation (1.11).

The relative performance of PAM-4 line coding improves at longer link lengths, as shown in Figures 1.12 and 1.13 for the case of a single link length of 150 m of the same Gaussian bandwidth multimode fiber. A qualitative eye opening measurement for both cases gives about the same value of 18 %, leading to a positive net gain of 1.5 dB, which coincides with the noise bandwidth enhancement factor. The breakeven point in using PAM-4 instead of NRZ for this Gaussian bandwidth multimode fiber is therefore somewhere between 100 m and 150 m, where the net gain is zero. For every longer link length, PAM-4 gives theoretically better performances than NRZ.

The last simulated case shown in Figures 1.14 and 1.15 refers to a single link length of 200 m of the same Gaussian bandwidth multimode fiber. The PAM-4 eye diagram looks almost closed, even
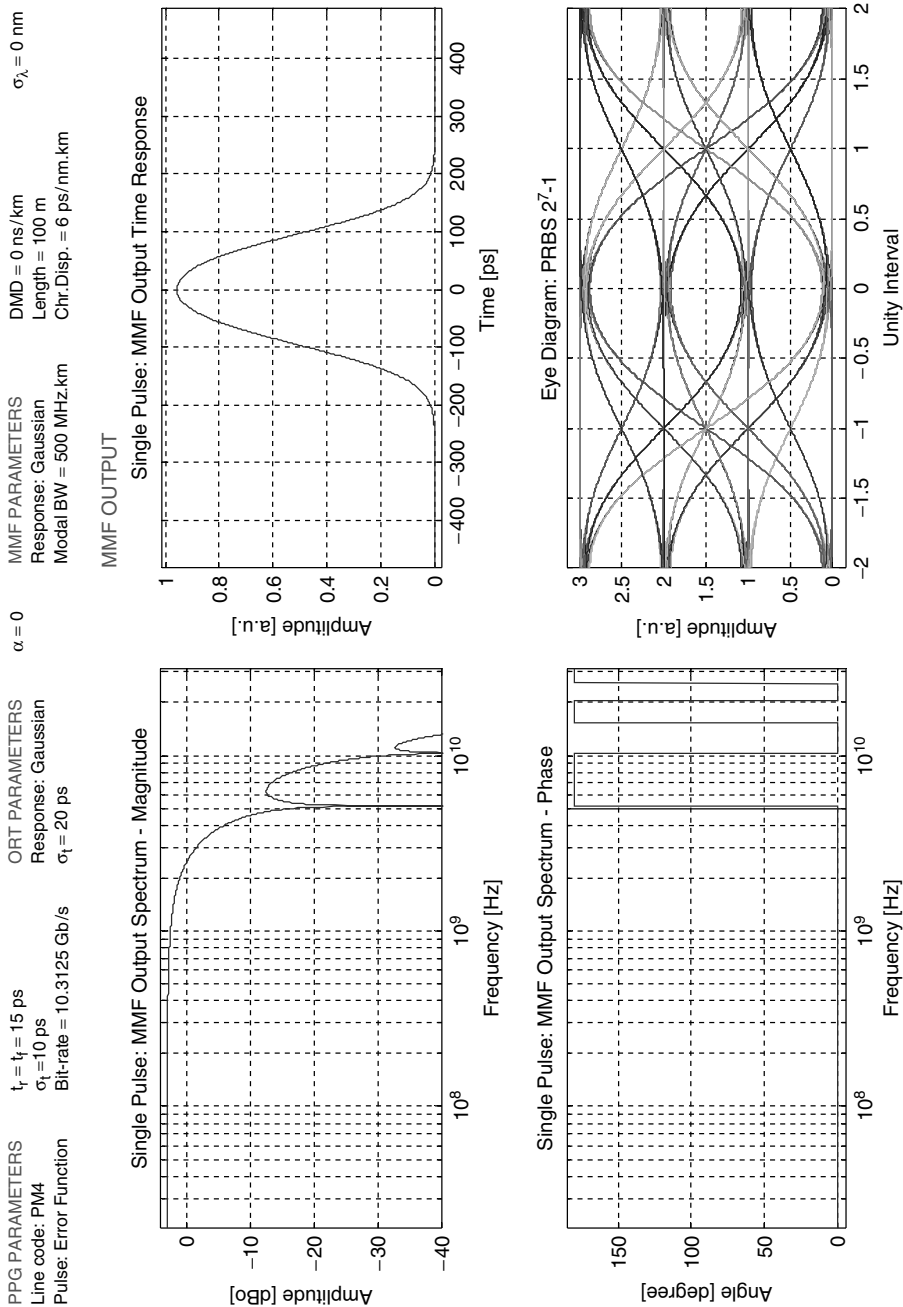
Figure 1.10 Frequency and time domain representations of PAM-4 PRBS 2^7-1 line code signals at 10GbE data rate after a 100 m single link length of Gaussian bandwidth multimode fiber. Left top represents the single pulse fiber output, while the left bottom graph shows the corresponding eye diagram in normalized bit time units. The legend at the top reports the simulated conditions for the pulse pattern generator and the light source impulse response
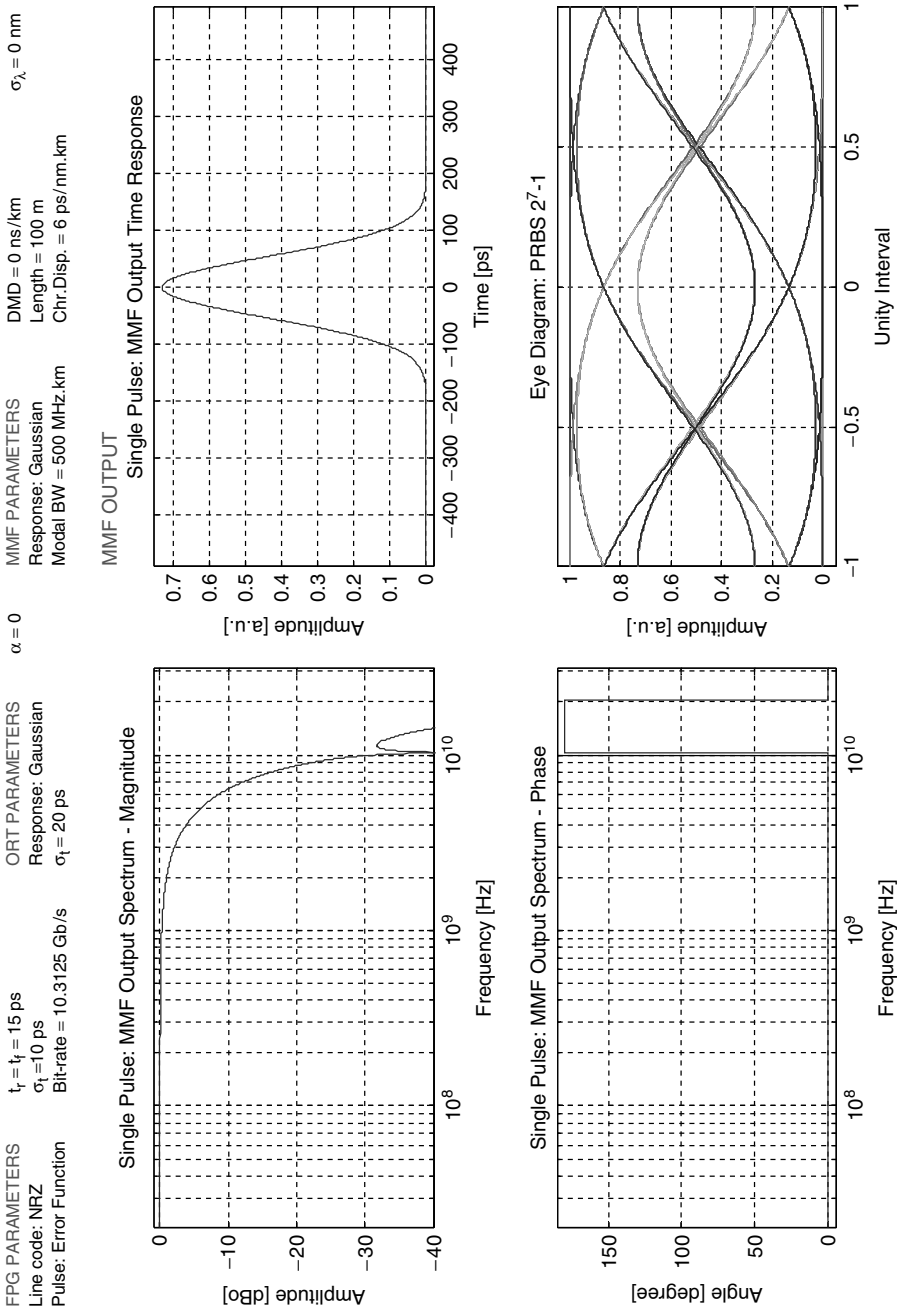
Figure 1.11 Frequency and time domain representations of NRZ PRBS 2^7-1 line code signals at 10GbE data rate after a 100 m single link length of Gaussian bandwidth multimode fiber. Left top represents the single pulse fiber output, while the left bottom graph shows the corresponding eye diagram in normalized bit time units. The legend at the top reports the simulated conditions for the pulse pattern generator and the light source impulse response
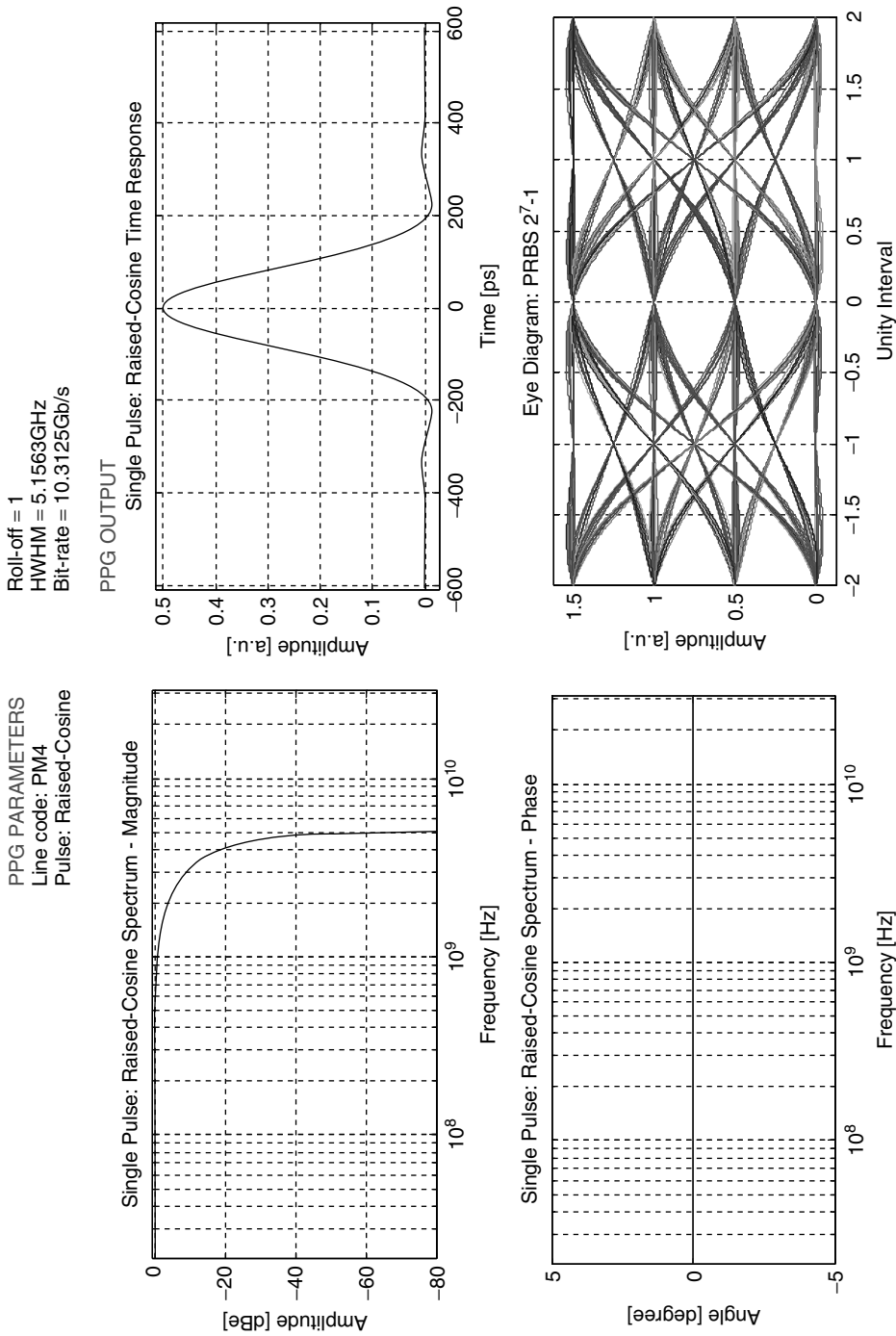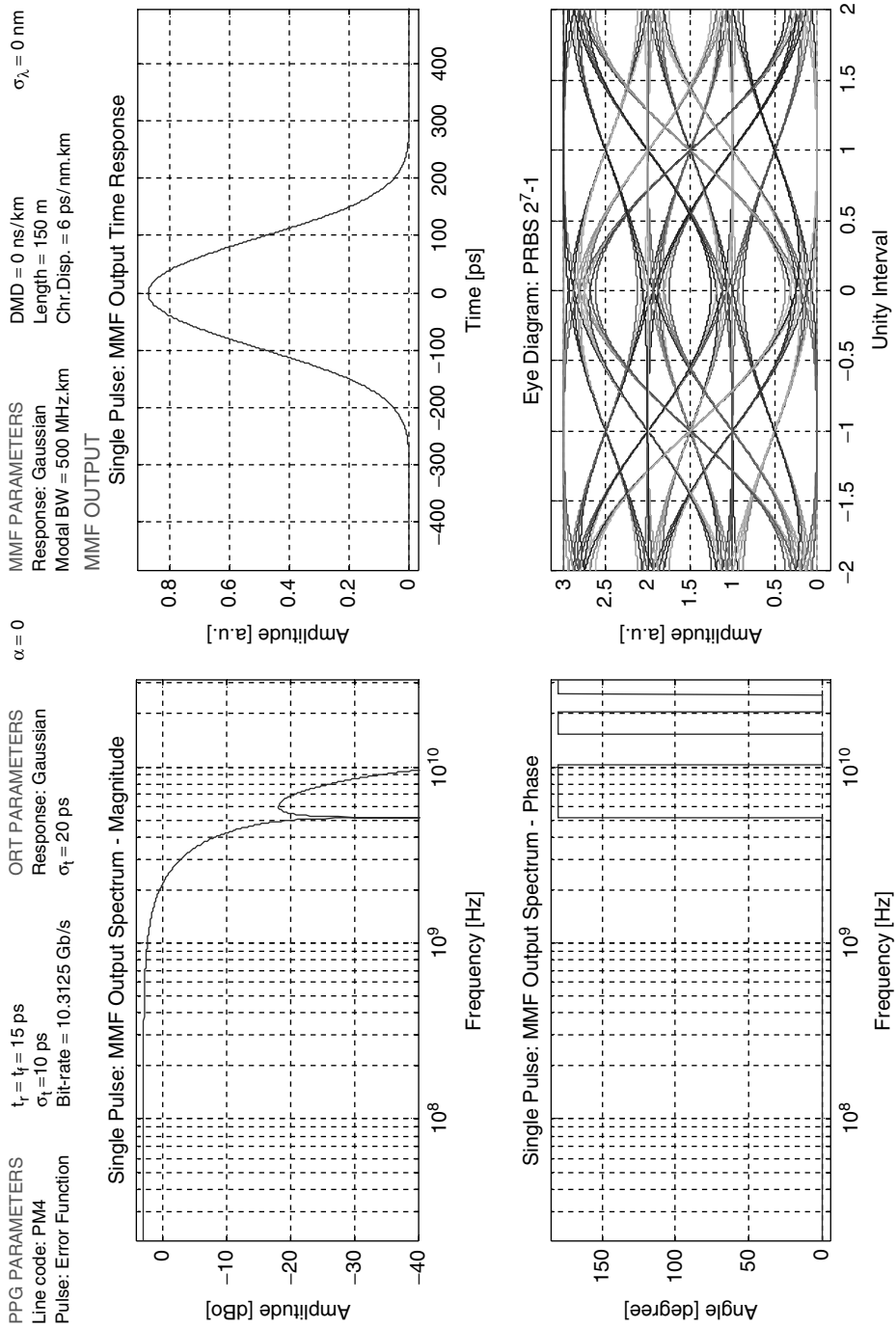
Figure 1.12 Frequency and time domain representations of PAM-4 PRBS 2^7-1 line code signals at 10GbE data rate after a 150 m single link length of Gaussian bandwidth multimode fiber. Left top represents the single pulse fiber output, while the left bottom graph shows the corresponding eye diagram in normalized bit time units. The legend at the top reports the simulated conditions for the pulse pattern generator and the light source impulse response
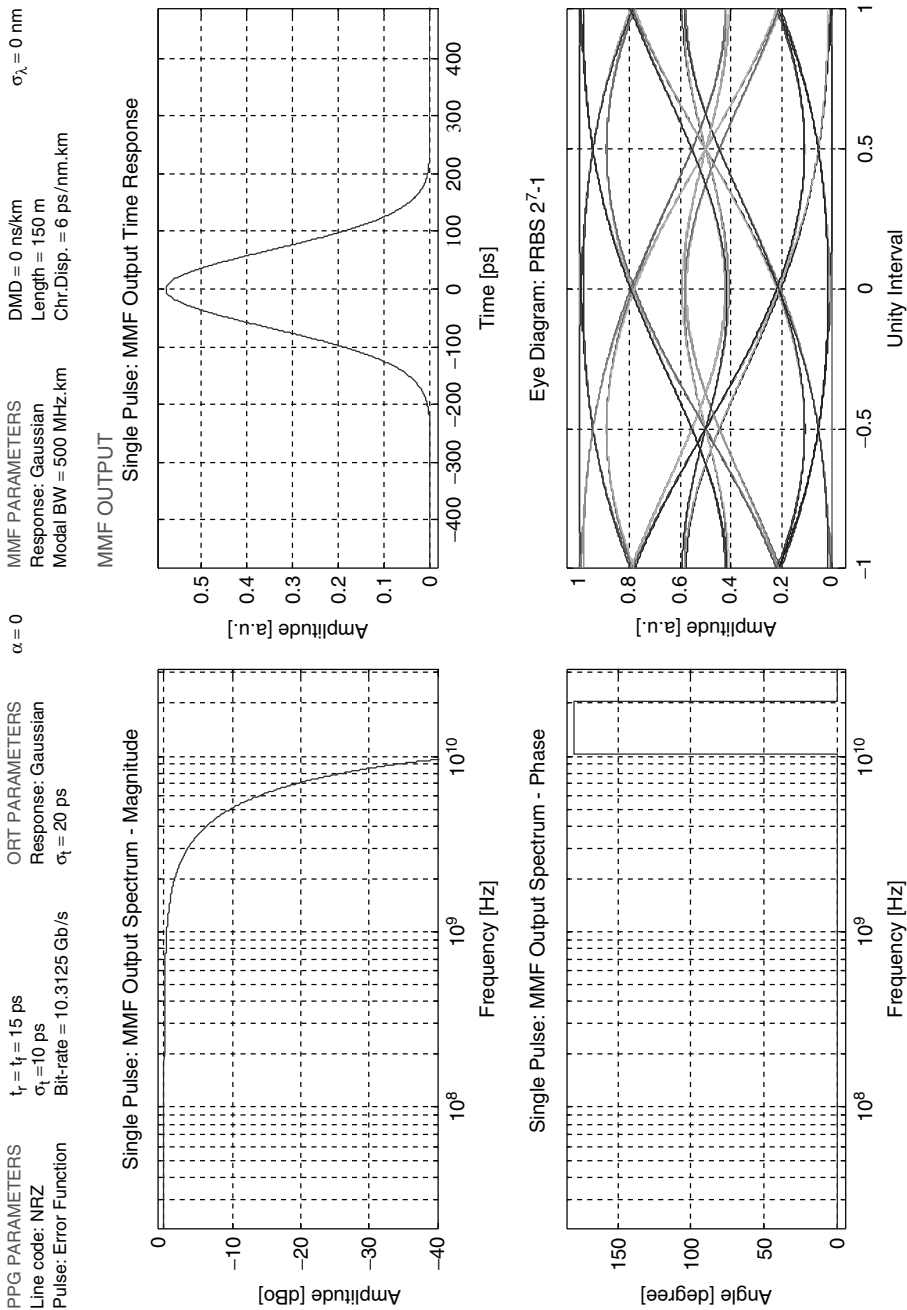
Figure 1.13 Frequency and time domain representations of NRZ PRBS 2^7-1 line code signals at 10GbE data rate after a 150 m single link length of Gaussian bandwidth multimode fiber. Left top represents the single pulse fiber output, while the left bottom graph shows the corresponding eye diagram in normalized bit time units. The legend at the top reports the simulated conditions for the pulse pattern generator and the light source impulse response
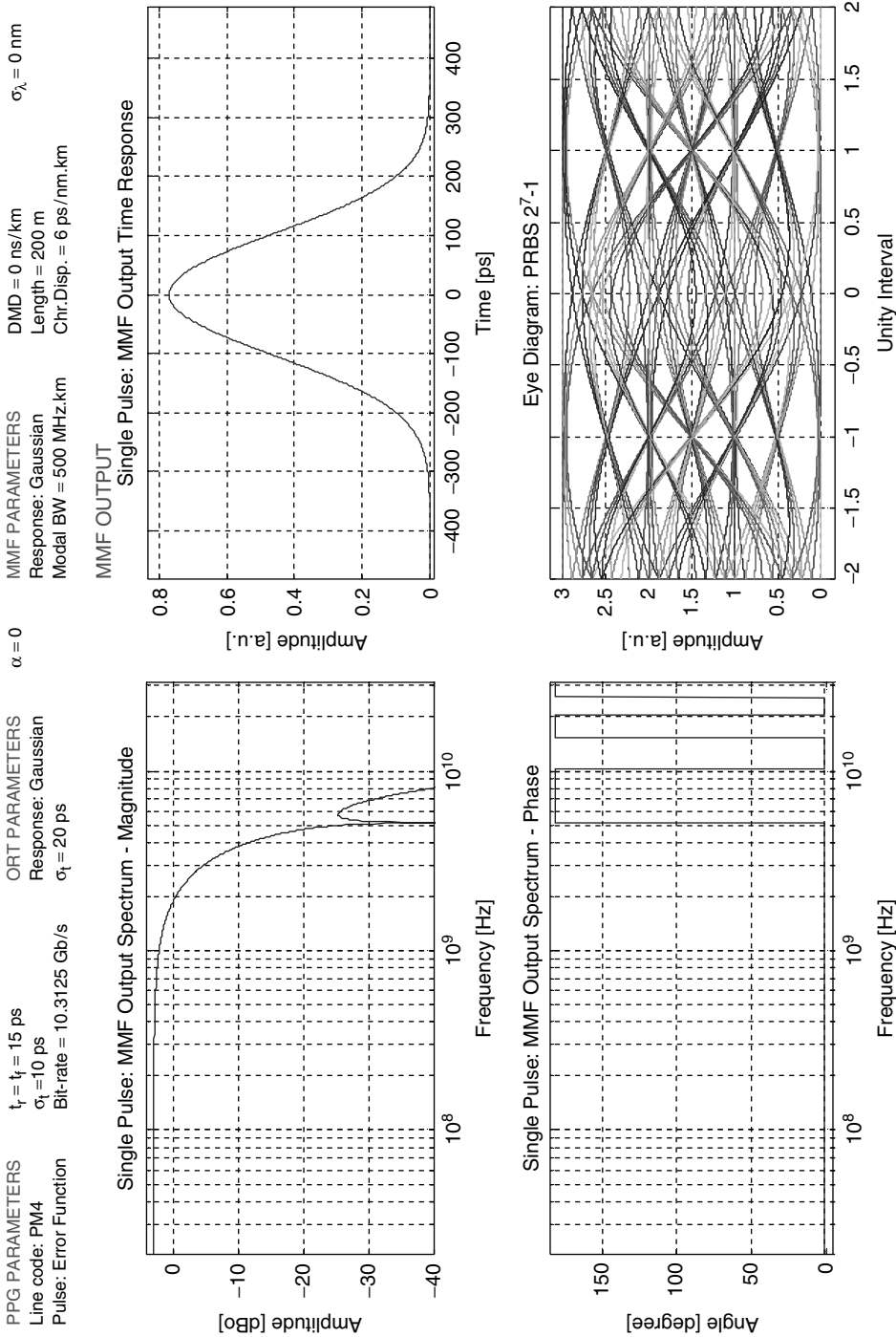
Figure 1.14 Frequency and time domain representations of PAM-4 PRBS 2^7-1 line code signals at 10GbE data rate after a 200 m single link length of Gaussian bandwidth multimode fiber. Left top represents the single pulse fiber output, while the left bottom graph shows the corresponding eye diagram in normalized bit time units. The legend at the top reports the simulated conditions for the pulse pattern generator and the light source impulse response
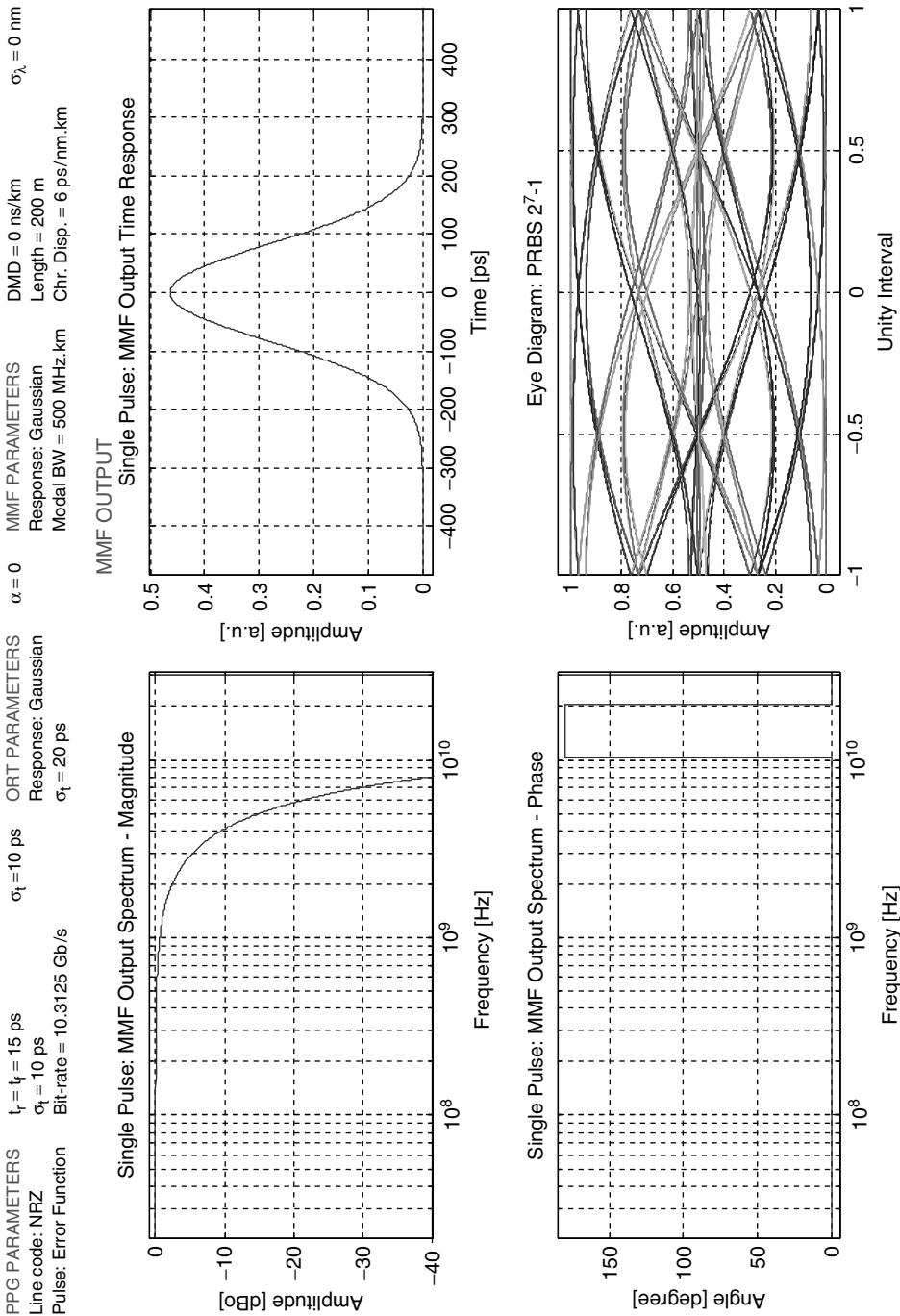
Figure 1.15 Frequency and time domain representations of NRZ PRBS 2^7-1 line code signals at 10GbE data rate after a 200 m single link length of Gaussian bandwidth multimode fiber. Left top represents the single pulse fiber output, while the left bottom graph shows the corresponding eye diagram in normalized bit time units. The legend at the top reports the simulated conditions for the pulse pattern generator and the light source impulse response

if small signal detection still seems possible. There is twice the channel bandwidth requirement in the case of NRZ coding, which leads instead to a completely closed eye diagram.

1.6.3.5 PAM-4 Coding Impairments in Optical Modulation

Previous analysis showed the comparison between NRZ and PAM-4 line code formats. The inherent reduced bandwidth occupancy of the PAM-4 line coding for the same information capacity supported by the NRZ format makes the former solution quite attractive as a valuable coding technique for overcoming the band-limited restrictions of legacy multimode fibers when operated at 10GbE standard. This is clearly summarized by the plot presented in Figure 1.7 between the coding net gain and the link distance for a given single multimode fiber. In that case, when the link length exceeds about 120 m, the PAM-4 coding results in superior performances with an increased signal-to-noise ratio. This is achieved by balancing the initially reduced eye opening due to multilevel modulation with the reduced signal pulse broadening during its propagation along the multimode fiber. The higher frequency content of the NRZ pulse undergoes a stronger interaction with the band-limited operation of the transmission channel, resulting in a relatively larger pulse dispersion.

These considerations are correct but they do not include any design issues or light source specifications. In order to obtain PAM-4 coding there is a need to discriminate among four different signal levels which correspond to three signal intervals. Figure 1.16 shows the PAM-4 signal and noise specifications.

The simple theory presented in the previous section assumes implicitly that the four signal levels are equally spaced and the noise power is uniform among them. This is reasonably true for
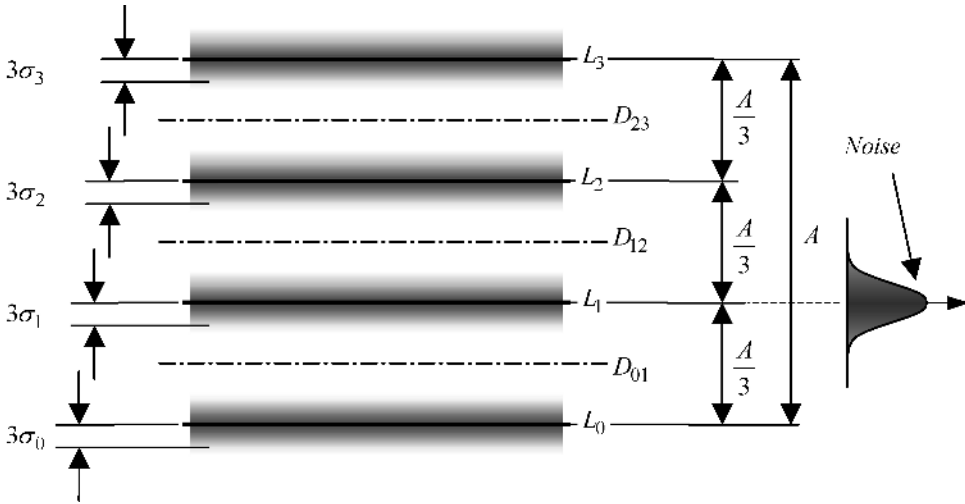
Figure 1.16 The PAM-4 code is represented through four digital levels, L_0, L_1, L_2, L_3, uniformly spaced by $A/3$, where $A = L_3 - L_0$ is the maximum signal amplitude. The noise level is qualitatively represented by $3\sigma_k$ and added over the signal level. Index $k = 0, 1, 2, 3$ indicates the corresponding signal level. Mid-range decision thresholds are respectively D_{01}, D_{12}, D_{23}

electrical PAM-4 modulation but it is not the general case for optical PAM-4 modulation. Different noise contributions on each signal level must be divided according to the source and the detector contribution. Depending on the detection system used, there may be either a negligible or a relevant shot noise contribution, and even a signal-spontaneous beat noise term if optical amplification is used at the receiver end section.

It is well known in optical communication that the shot noise power is proportional to the signal average optical power leading to an increasing signal-to-noise ratio as the square root of the average received optical power. In the case of optically amplified transmission systems, the signal-spontaneous beat noise usually becomes the dominant noise term and the signal-to-noise ratio remains constant versus the received average optical power, which leads to the well-known optical signal-to-noise ratio (OSNR) limited operations. Since both shot noise and signal-spontaneous beat noise are dependent on the optical signal level, it might be expected that optical PAM-4 exhibits a decreasing signal-to-noise ratio moving from the lower signal level towards the higher signal level. This could be compensated by properly adjusting the decision threshold for every signal interval. It this case, moving from the lowest interval towards a higher one, the decision threshold must be positioned correspondingly below the mid-range position, at relatively decreasing distances from the lower signal level. This threshold adjustment will compensate for higher noise fluctuations on the higher signal level.

There is at least one more reason for having different decision conditions corresponding to different intervals in the PAM-4 signal structure shown in Figure 1.16, namely the nonlinearity of the laser source transfer characteristic and the quite different source noise added to different levels due to strong differences in the lasing conditions. Laser nonlinearities in the L-I (eight power−current intensity) characteristic are responsible for different interval amplitudes between consecutive signal levels. Compared to the NRZ line coding, the reduced interval amplitude together with the laser nonlinearities makes the PAM-4 line coding implementation at 10GbE a very challenging design. In addition, the different noise spectral power densities exhibited by every direct modulated laser source at different lasing intensities require a careful decision threshold design. It will be seen later in this book that the optimum decision threshold between any two digital signal levels is determined by the minimum error probability achievable for the given signal amplitude and noise distributions on both levels. If noise distribution is not the same or if it changes during the lasing life, the corresponding optimum decision would require an adaptive threshold capability.

1.6.3.6 EDC-Based PAM-4 to NRZ Decoder

Figure 1.17 shows qualitatively the block diagram for an EDC-based PAM-4 decoder to be used in 10GbE transmission over legacy multimode fiber. The optical line code is assumed to be PAM-4 running at 10.3125 Gb/s. The optical detector followed by the low-noise transimpedance amplifier provides linear conversion to PAM-4 in the electrical domain. This signal simultaneously feeds the three binary signal discriminators operating at the equivalent half-rate NRZ line code. The embedded EDC feature improves the signal recognition after fiber bandwidth limitation added significant distortion. It is important to remark that the electrical signal speed in each discriminator is just half a bit rate, then 5.15625 Gb/s. This makes EDC implementation easier using the same high-speed IC technology as that used for the low-noise front end. Once the signal has been first discriminated among the three possible intervals defined by the PAM-4 coding, the LOGIC block provides the NRZ data coding.
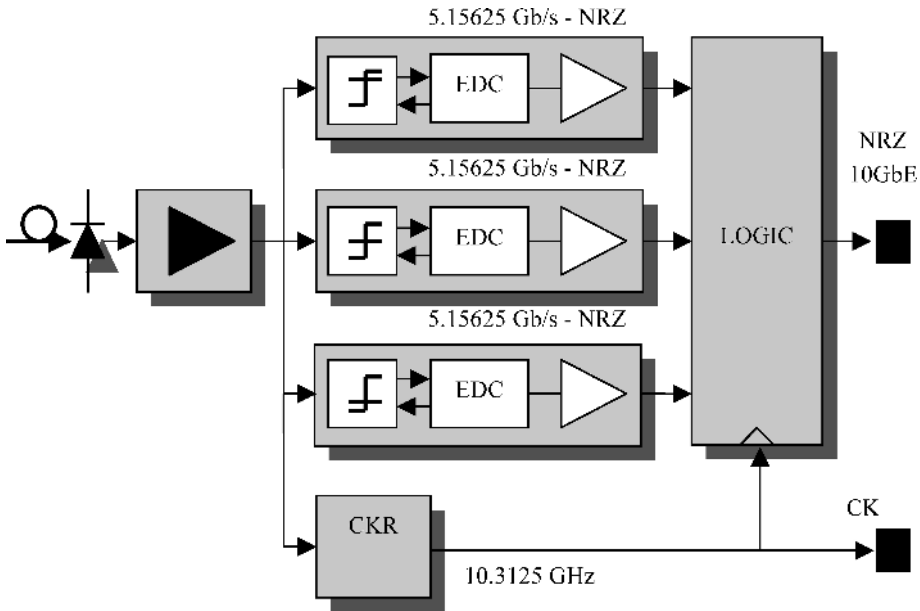
Figure 1.17 Block diagram of the EDC-based PAM-4 receiver. The optical signal is first detected assuming a linear PAM-4 transimpedance amplifier. Then each of the three signal discriminators operates according to the selected threshold with the EDC feature. The LOGIC block provides the NRZ coding output. The required signal speed of each signal discriminator is just one-half of the equivalent NRZ line code

1.7 Conclusions and Recommendations

The three solutions presented so far, namely EDC, OMF and PAM-4, serve as mitigating countermeasures for multimode fiber bandwidth limitation. In principle all these three solutions should allow 10GbE transmission over long-reach multimode fiber, although EDC gains an advantageous position due to the intense development pursued by several IC companies involved in these projects. Electronic dispersion compensation now looks much more promising than the other two alternatives, mainly due to relatively more relaxed optical tolerances required by the fiber channel and the laser source. Although at the present time a solid EDC design capable of successfully linking 300 m of legacy multimode fiber under operating field conditions has not yet been demonstrated, many laboratory experiments have demonstrated its compensation capability, including dynamic multipath adaptations.

In the following some general recommendations are summarized for achieving a successful 10GbE transmission over a multimode fiber link:

1. The 10GbE system must work with legacy MMF. No old fiber replacement should be planned.
2. No special patchcord should be used for restricted launching conditions. Those items will add cost and bulky passive components to the system layout. An integrated offset launching tool should be recommended for high-volume and low-cost production.
3. Low-cost and directly modulated receptacle laser sources must be used, instead of better performing but much more expensive solutions. More sophisticated transmitter solutions using externally modulated laser sources, such as the EAM-DFB laser, do not match both cost requirement and reduced power consumption for high-density pluggable modules. VCSEL, Fabry-Perot (FP) or

Table 1.1 Optical fiber telecommunication standards operating at the bit rate range of 155 Mb/s

Standards	Nominal Rate (Mb/s)	Recommendation	Application	Module MSA	Code	Bit rate (Mb/s)	Fiber	Distance (km)	Nominal WL (nm)	WL range (nm)	Attenuation range (dB)	CD max (ps/nm)	Penalty (dB)	Source	Linewidth RMS (nm)	PSD max (mW/MHz)	PWR range (dBm)	ER (dB)	SMSR (dB)	Detector	ESNR (dB10)	Sensitivity (dBm)	OVL (dBm)	BER
OC-1	51 M	Telcordia GR-253 CORE	Telecom	–	SR-1	51840	SM-G.652	12	1310	1260–1360	0–7	NA	1	MLM-FP-VCSEL	80	NA	–23/–14	8.2	NA	PIN	ffs	–31	–14	1.0×10^{-10}
														LED		NA			NA	PIN	ffs		–8	1.0×10^{-10}
					IR-1	51840	SM-G.652	21	1310	1260–1360	0–12	96	1	MLM-FP-VCSEL	23	NA	–15/–8	8.2	NA	PIN	ffs	–28	–8	1.0×10^{-10}
					IR-2	51840	SM-G.652	42	1550	1430–1580	0–12	317	1	MLM-FP-VCSEL	4	NA	–15/–8	8.2	NA	PIN	ffs	–28	–8	1.0×10^{-10}
												NA		SLM-DFB/DM	1 at –20dB	ffs			30	PIN	ffs			1.0×10^{-10}
					LR-1	51840	SM-G.652	50	1310	1280–1335	10–28	171	1	MLM-FP-VCSEL	13	NA	–5/0	10	NA	PIN	ffs	–34	–10	1.0×10^{-10}
												NA		SLM-DFB/DM	1 at –20dB	ffs			30	PIN	ffs			1.0×10^{-10}
					LR-2	51840	SM-G.652	100	1550	1480–1580	10–28	20	1	SLM-DFB/DM	1 at –20dB	ffs	–5/0	10	30	PIN	ffs	–34	–10	1.0×10^{-10}
					LR-3	51840	SM-G.653	100	1550	1480–1580	10–28	444	1	MLM-FP-VCSEL	5	NA	–5/0	10	NA	PIN	ffs	–34	–10	1.0×10^{-10}
												NA		SLM-DFB/DM	1 at –20dB	ffs			30	PIN	ffs			1.0×10^{-10}
STM-1	155 M	ITU-T G.957	Telecom	–	I-1	155520	SM-G.652	2	1310	1260–1360	0–7	18	1	MLM-FP-VCSEL	40	NA	–15/–8	8.2	NA	PIN	ffs	–23	–8	1.0×10^{-10}
												25		LED	80	NA			NA	PIN	ffs		–8	1.0×10^{-10}
					S-1.1	155520	SM-G.652	15	1310	1260–1360	0–12	96	1	MLM-FP-VCSEL	7.7	NA	–15/–8	8.2	NA	PIN	ffs	–28	–8	1.0×10^{-10}
					S-1.2	155520	SM-G.652	15	1550	1430–1576	0–12	296	1	MLM-FP-VCSEL	2.5	NA	–15/–8	8.2	NA	PIN	ffs	–28	–8	1.0×10^{-10}
										1430–1580		NA		SLM-DFB/DM	1 at –20dB	ffs			30	PIN	ffs			1.0×10^{-10}
					L-1.1	155520	SM-G.652	40	1310	1263–1360	10–28	246	1	MLM-FP-VCSEL	3	NA	–5/0	10	NA	PIN	ffs	–34	–10	1.0×10^{-10}
												NA		SLM-DFB/DM	1 at –20dB	ffs			30	PIN	ffs			1.0×10^{-10}
					L-1.2	155520	SM-G.652/G.654	80	1550	1480–1580	10–28	NA	1	SLM-DFB/DM	1 at –20dB	ffs	–5/0	10	30	PIN	ffs	–34	–10	1.0×10^{-10}
										1534–1566		246		MLM-FP	3				NA			–10		
					L-1.3	155520	SM-G.653	80	1550	1523–1577	10–28	296	1	SLM-DFB/DM	2.5	ffs	–5/0	10	NA	PIN	ffs	–34	–10	1.0×10^{-10}
										1480–1580		NA		SLM-DFB/DM	1 at –20dB				30					1.0×10^{-10}

Table 1.1 (*continued*)

Standards	Nominal Rate (Mb/s)	Recommendation	Application	Module MSA	Code	Bit rate (Mb/s)	Fiber	Distance (km)	Nominal WL (nm)	WL range (nm)	Attenuation range (dB)	CD max (ps/nm)	Penalty (dB)	Source	Linewidth RMS (nm)	PSD max (mW/MHz)	PWR range (dBm)	ER (dB)	SMSR (dB)	Detector	ESNR (dB10)	Sensitivity (dBm)	OVL (dBm)	BER
OC-1 55M / STM-3		Telecordia		–	SR-1	155 520	SM-G.652	12	1310	1260–1360	0–7	18	1	MLM-FP-VCSEL	40	NA	−15/−8	8.2	NA	PIN	ffs	−23	−8	1.0×10^{-10}
												25		LED	80				NA					1.0×10^{-10}
					IR-1	155 520	SM-G.652	21	1310	1261–1360	0–12	96	1	MLM-FP-VCSEL	7.7	NA	−15/−8	8.2	NA	PIN	ffs	−28	−8	1.0×10^{-10}
					IR-2	155 520	SM-G.652	42	1550	1430–1576	0–12	296	1	MLM-FP-VCSEL	2.5	NA	−15/−8	8.2	NA	PIN	ffs	−28	−8	1.0×10^{-10}
										1430–1580		NA		SLM-DFB/DM	1 at −20dB	ffs			30					1.0×10^{-10}
		GR-253 CORE			LR-1	155 520	SM-G.652	50	1310	1263–1360	10–28	246	1	MLM-FP-VCSEL	3	NA	−5/0	10	NA	PIN	ffs	−34	−10	1.0×10^{-10}
												NA		SLM-DFB/DM	1 at −20dB	ffs			30					1.0×10^{-10}
					LR-2	155 520	SM-G.652	100	1550	1480–1580	10–28	20	1	SLM-DFB/DM	1 at −20dB	ffs	−5/0	10	30	PIN	ffs	−34	−10	1.0×10^{-10}
					LR-3	155 520	SM-G.653	100	1550	1534–1566	10–28	246		MLM-FP-VCSEL	3	NA	−5/0	10	NA	PIN	ffs	−34	−10	1.0×10^{-10}
										1523–1577		296	1	MLM-FP-VCSEL	2.5				NA					1.0×10^{-10}
										1480–1580		NA		SLM-DFB/DM	1 at −20dB	ffs			30					1.0×10^{-10}

Table 1.2 Optical fiber telecommunication standards operating at the bit rate range of 622 Mb/s and 2.5 Gb/s

FO standards	Nominal rate (Mb/s)	Recommendation	Application	Code	Bit rate (Mb/s)	Fiber	Distance (km)	Nominal WL (nm)	WL range (nm)	Attenuation range (dB)	CD_max (ps/nm)	Penalty (dB)	Source	Linewidth RMS (nm)	SPD_max (mW/MHz)	PWR range (dBm)	ER (dB)	SMSR (dB)	Detector	ESNR (dB10)	Sensitivity (dBm)	OVL (dBm)	BER
STM-4	622 M	ITU-T G.957	Telecom	I-4	622 080	SM-G.652	2	1310	1261–1360	0–7	13 / 14	1	MLM-FP-VCSEL / LED	14.5 / 35	NA	−15/−8	8.2	NA	PIN	ffs	−23	−8	1.0×10^{-10} / 1.0×10^{-10}
				S-4.1	622 080	SM-G.652	15	1310	1293–1334 / 1274–1356	0–12	46 / 74	1	MLM-FP-VCSEL	4 / 2.5	NA	−15/−8	8.2	NA	PIN	ffs	−28	−8	1.0×10^{-10}
				S-4.2	622 080	SM-G.652	15	1550	1430–1580	0–12	NA	1	SLM-DFB/DM	1 at −20dB	ffs	−15/−8	8.2	30	PIN	ffs	−28	−8	1.0×10^{-10}
				L-4.1	622 080	SM-G.652	40	1310	1300–1325 / 1296–1330 / 1280–1335	10–24	92 / 109 / NA	1	MLM-FP-VCSEL / SLM-DFB/DM	2 / 1.7 / 1 at −20dB	NA / ffs	−3/+2	10	NA / 30	PIN	ffs	−28	−8	1.0×10^{-10} / 1.0×10^{-10} / 1.0×10^{-10}
				L-4.2	622 080	SM-G.652/ G.654	80	1550	1480–1580	10–24	NA	1	SLM-DFB/DM	1 at −20dB	ffs	−3/+2	10	30	PIN	ffs	−28	−8	1.0×10^{-10}
				L-4.3	622 080	SM-G.653	80	1550	1480–1580	10–24	NA	1	SLM-DFB/DM	1 at −20dB	ffs	−3/+2	10	30	PIN	ffs	−28	−8	1.0×10^{-10}
STM-4	622 M	ITU-T G.691	Telecom	V-4.1	622 080	SM-G.652	60	1310	1290–1330	22–33	200	1	SLM-DFB/DM	ffs	ffs	0/+4	10	ffs	PIN/APD	ffs	−34	−18	1.0×10^{-12}
				V-4.2	622 080	SM-G.652	120	1550	1530–1565	22–33	2,400	1	SLM-DFB/DM	ffs	ffs	0/+4	10	ffs	PIN/APD	ffs	−34	−18	1.0×10^{-12}
				V-4.3	622 080	SM-G.653	120	1550	1530–1565	22–33	400	1	SLM-DFB/DM	ffs	ffs	0/+4	10	ffs	PIN/APD	ffs	−34	−18	1.0×10^{-12}
				U-4.2	622 080	SM-G.652	160	1550	1530–1565	33–44	3,200	2	SLM-DFB/EM	ffs	ffs	+12/+15	10	ffs	PIN/APD	ffs	−34	−18	1.0×10^{-12}
				U-4.3	622 080	SM-G.653	160	1550	1530–1565	33–44	530	1	SLM-DFB/EM	ffs	ffs	+12/+15	10	ffs	PIN/APD	ffs	−33	−18	1.0×10^{-12}
OC-12	622 M	Telcordia GR-253-CORE	Telecom	SR-1	622 080	SM-G.652	12	1310	1261–1360	0–7	13 / 14	1	MLM-FP-VCSEL / LED	14.5 / 35	NA	−15/−8	8.2	NA	PIN	ffs	−23	−8	1.0×10^{-10} / 1.0×10^{-10}
				IR-1	622 080	SM-G.652	21	1310	1293–1334 / 1274–1356	0–12	46 / 74	1	MLM-FP-VCSEL	4 / 2.5	NA	−15/−8	8.2	NA	PIN	ffs	−28	−8	1.0×10^{-10}
				IR-2	622 080	SM-G.652	42	1550	1430–1580	0–12	NA	1	SLM-DFB/DM	1 at −20dB	ffs	−15/−8	8.2	30	PIN	ffs	−28	−8	1.0×10^{-10}
				LR-1	622 080	SM-G.652	42	1310	1300–1325 / 1296–1330 / 1280–1335	10–24	92 / 109 / NA	1	MLM-FP-VCSEL / SLM-DFB/DM	2 / 1.7 / 1 at −20dB	NA / ffs	−3/+2	10	NA / 30	PIN	ffs	−28	−8	1.0×10^{-10} / 1.0×10^{-10} / 1.0×10^{-10}
				LR-2	622 080	SM-G.652	85	1550	1480–1580	10–24	NA	1	SLM-DFB/DM	1 at −20dB	ffs	−3/+2	10	30	PIN	ffs	−28	−8	1.0×10^{-10}
				LR-3	622 080	SM-G.653	85	1550	1480–1580	10–24	NA	1	SLM-DFB/DM	1 at −20dB	ffs	−3/+2	10	30	PIN	ffs	−28	−8	1.0×10^{-10}

(continued overleaf)

Table 1.2 (*continued*)

FO standards	Nominal rate (Mb/s)	Recommendation	Application	Code	Bit rate (Mb/s)	Fiber	Distance (km)	Nominal WL (nm)	WL range (nm)	Attenuation range (dB)	CD$_{max}$ (ps/nm)	Penalty (dB)	Source	Linewidth RMS (nm)	SPD$_{max}$ (mW/MHz)	PWR range (dBm)	ER (dB)	SMSR (dB)	Detector	ESNR (dB10)	Sensitivity (dBm)	OVL (dBm)	BER
STM-16	2.6G	ITU-T G.957	Telecom 300	I-16	2488 320	SM-G.652	2	1310	1266–1360	0–7	12	1	MLM-FP-VCSEL	4	NA	−10/−3	8.2	NA	PIN	ffs	−18	−3	1.0 × 10^{-10}
				S-16.1	2488 320	SM-G.652	15	1310	1260–1360	0–12	NA	1	SLM-DFB/DM	1 at −20dB	ffs	−5/0	8.2	30	PIN	ffs	−18	0	1.0 × 10^{-10}
				S-16.2	2488 320	SM-G.653	15	1550	1430–1580	0–12	NA	1	SLM-DFB/DM	<1 at −20dB	ffs	−5/0	8.2	30	PIN	ffs	−18	0	1.0 × 10^{-10}
				L-16.1	2488 320	SM-G.652	40	1310	1280–1335	10–24	NA	1	SLM-DFB/EM	1 at −20dB	ffs	−2/+3	8.2	30	PIN	ffs	−27	−9	1.0 × 10^{-10}
				L-16.2	2488 320	SM-G.652/G.654	80	1550	1500–1580	10–24	1200–1600	1	SLM-DFB/EM	<1 at −20dB	ffs	−2/+3	8.2	30	PIN	ffs	−28	−9	1.0 × 10^{-10}
				L-16.3	2488 320	SM-G.653	80	1550	1500–1580	10–24	NA	1	SLM-DFB/EM	1 at −20dB	ffs	−2/+3	8.2	30	PIN	ffs	−27	−9	1.0 × 10^{-10}
	2.6G	ITU-T G.691	Telecom	V-16.2	2488 320	SM-G.652	120	1550	1530–1565	22–33	2,400	2	SLM-DFB/EM	ffs	ffs	+10/+13	8.2	ffs	PIN/APD	ffs	−25	−9	1.0 × 10^{-12}
				V-16.3	2488 320	SM-G.653	120	1550	1530–1565	22–33	400	1	SLM-DFB/EM	ffs	ffs	+10/+13	8.2	ffs	PIN/APD	ffs	−24	−9	1.0 × 10^{-12}
				U-16.2	2488 320	SM-G.652	160	1550	1530–1565	33–44	3,200	2	SLM-DFB/EM	ffs	ffs	+12/+15	10	ffs	APD	ffs	−34	−18	1.0 × 10^{-12}
				U-16.3	2488 320	SM-G.653	160	1550	1530–1565	33–44	530	1	SLM-DFB/EM	ffs	ffs	+12/+15	10	ffs	APD	ffs	−33	−18	1.0 × 10^{-12}
OC-48	2.6G	Telcordia GR-253	Telecom	SR-1	2488 320	SM-G.652	12	1310	1266–1360	0–7	12	1	MLM-FP-VCSEL	4	NA	−10/−3	8.2	NA	PIN	ffs	−18	−3	1.0 × 10^{-10}
				IR-1	2488 320	SM-G.652	21	1310	1260–1360	0–12	NA	1	SLM-DFB/DM	1 at −20dB	ffs	−5/0	8.2	30	PIN	ffs	−18	0	1.0 × 10^{-10}
				IR-2	2488 320	SM-G.652	42	1550	1430–1580	0–12	ffs	1	SLM-DFB/DM	<1 at −20dB	ffs	−5/0	8.2	30	PIN	ffs	−18	0	1.0 × 10^{-10}
				LR-1	2488 320	SM-G.652	42	1310	1280–1335	10–24	NA	1	SLM-DFB/EM	1 at −20dB	ffs	−2/+3	8.2	30	PIN	ffs	−27	−9	1.0 × 10^{-10}
				LR-2	2488 320	SM-G.652	85	1550	1500–1580	10–24	1200–1600	2	SLM-DFB/EM	<1 at −20dB	ffs	−2/+3	8.2	30	PIN	ffs	−28	−9	1.0 × 10^{-10}
				LR-3	2488 320	SM-G.653	85	1550	1500–1580	10–24	NA	1	SLM-DFB/DM	1 at −20dB	ffs	−2/+3	8.2	30	PIN	ffs	−27	−9	1.0 × 10^{-10}

Table 1.3 Optical fiber telecommunication standards operating at the bit rate range of 10 Gb/s

Code	Bit rate (Mb/s)	Fiber	Distance (km)	Nominal WL (nm)	WL range (nm)	Attenuation range (dB)	CD_{max} (ps/nm)	Penalty (dB)	Source	Linewidth RMS (nm)	SPD_{max} (mW/MHz)	PWR range (dBm)	ER (dB)	SMSR (dB)	Detector	ESNR (dB10)	Sensitivity (dBm)	OVL (dBm)	BER
VSR600-2M1	9 953 280	SM-G.652	0.6	1310	1260–1360	3–12	4	1	MLM-FP-VCSEL	3	NA	+2/+5	6	NA	PIN	ffs	−11	−1	1.0×10^{-12}
VSR600-2M2	9 953 280	SM-G.652	0.6	1550	1530–1565	3–12	12	1	MLM-FP-VCSEL	NA	NA	−1/+2	8.2	30	PIN	ffs	−14	−1	1.0×10^{-12}
VSR600-2M5	9 953 280	SM-G.655	0.6	1550	1530–1565	3–12	10	1	MLM-FP-VCSEL	NA	NA	−1/+2	8.2	30	PIN	ffs	ffs	ffs	1.0×10^{-12}
I-64.1r	9953280	SM-G.652	0.6	1310	1260–1360	0–4	4	1	MLM-FP-VCSEL	3	NA	−6/−1	6	NA	PIN	ffs	−11	−1	1.0×10^{-12}
I-64.1	9953280	SM-G.652	2	1310	1290–1330	0–4	7	1	SLM-DFB	<1 at −20dB	ffs	−6/−1	6	30	PIN	ffs	−11	−1	1.0×10^{-12}
I-64.2r	9953280	SM-G.652	2	1550	1530–1565	0–7	40	2	SLM-DFB	ffs	ffs	−5/−1	8.2	30	PIN	ffs	−14	−1	1.0×10^{-12}
I-64.2	9953280	SM-G.652	25	1550	1530–1565	0–7	500	2	SLM-DFB/EM	ffs	ffs	−5/−1	8.2	30	PIN	ffs	−14	−1	1.0×10^{-12}
I-64.3	9953280	SM-G.653	25	1550	1530–1565	0–7	80	1	SLM-DFB/EM	ffs	ffs	−5/−1	8.2	30	PIN	ffs	−13	−1	1.0×10^{-12}
I-64.5	9953280	SM-G.655	25	1550	1530–1565	0–7	ffs	1	SLM-DFB/EM	ffs	ffs	−5/−1	8.2	30	PIN	ffs	−13	−1	1.0×10^{-12}
S-64.1	9953280	SM-G.652	20	1310	1290–1330	6–11	70	1	SLM-DFB/EM	ffs	ffs	+1/+5	6	30	PIN	ffs	−11	−1	1.0×10^{-12}
S-64.2a	9953280	SM-G.652	40	1550	1530–1565	7–11	800	2	SLM-DFB/EM	ffs	ffs	+5/−1	8.2	30	PIN/APD	ffs	−18	−8	1.0×10^{-12}
S-64.2b	9953280	SM-G.652	40	1550	1530–1565	3–11	800	2	SLM-DFB/EM	ffs	ffs	−1/+2	6	30	PIN	ffs	−14	−1	1.0×10^{-12}
S-64.3a	9953280	SM-G.653	40	1550	1530–1565	7–11	130	1	SLM-DFB/EM	ffs	ffs	+5/−1	8.2	30	PIN/APD	ffs	−17	−8	1.0×10^{-12}
S-64.3b	9953280	SM-G.653	40	1550	1530–1565	3–11	130	1	SLM-DFB/EM	ffs	ffs	−1/+2	6	30	PIN	ffs	−13	−1	1.0×10^{-12}
S-64.5a	9953280	SM-G.655	40	1550	1530–1565	7–11	130	1	SLM-DFB/EM	ffs	ffs	+5/−1	8.2	30	PIN/APD	ffs	−17	−8	1.0×10^{-12}
S-64.5b	9953280	SM-G.655	40	1550	1530–1565	3–11	130	1	SLM-DFB/EM	ffs	ffs	−1/+2	6	30	PIN	ffs	−13	−1	1.0×10^{-12}
L-64.1	9953280	SM-G.652	40	1310	1290–1320	17–22	130	1	SLM-DFB	ffs	ffs	+4/+7	6	30	APD	ffs	−19	−10	1.0×10^{-12}
L-64.2a	9953280	SM-G.652	80	1550	1530–1565	11–22	1,600	2	SLM-DFB	ffs	ffs	−2/+2	10	30	PIN/OA	ffs	−26	−9	1.0×10^{-12}
L-64.2b	9953280	SM-G.652	80	1550	1530–1565	16–22	1,600	2	SLM-DFB/EM	ffs	ffs	+10/+13	8.2	ffs	PIN	ffs	−14	−3	1.0×10^{-12}
L-64.2c	9953280	SM-G.652	80	1550	1530–1565	11–22	1,600	2	SLM-DFB/EM	ffs	ffs	−2/+2	10	ffs	PIN/OA	ffs	−26	−3	1.0×10^{-12}
L-64.3	9953280	SM-G.653	80	1550	1530–1565	16–22	260	1	SLM-DFB/EM	ffs	ffs	+10/+13	8.2	ffs	PIN	ffs	−13	−3	1.0×10^{-12}
V-64.2a	9953280	SM-G.652	120	1550	1530–1565	22–33	2,400	2	SLM-DFB/EM	ffs	ffs	+10/+13	10	ffs	PIN/OA	ffs	−25	−9	1.0×10^{-12}
V-64.2b	9953280	SM-G.652	120	1550	1530–1565	22–33	2,400	2	SLM-DFB/EM	ffs	ffs	+12/+15	10	ffs	PIN/OA	ffs	−23	−7	1.0×10^{-12}
V-64.3	9953280	SM-G.653	120	1550	1530–1565	22–33	400	1	SLM-DFB/EM	ffs	ffs	+10/+13	8.2	ffs	PIN/OA	ffs	−24	−9	1.0×10^{-12}
SR-1	9953280	SM-G.652	7	1310	1290–1330	0–4	6.6	1	SLM-DFB/DM	ffs	0.1	−6/−1	6	ffs	PIN	26	−11	−1	1.0×10^{-12}
SR-2	9953280	SM-G.652	25	1550	1530–1565	0–7	500	2	SLM-DFB/DM	ffs	0.1	−5/−1	8.2	ffs	PIN	26	−14	−1	1.0×10^{-12}
IR-1	9953280	SM-G.652	20	1310	1290–1330	6–11	70	1	SLM-DFB/EM	ffs	0.1	+1/+5	6	ffs	PIN	26	−11	−1	1.0×10^{-12}
IR-2	9953280	SM-G.652	40	1550	1530–1565	6–11	800	2	SLM-DFB/EM	ffs	0.1	−1/+2	8.2	ffs	PIN	26	−14	−1	1.0×10^{-12}
IR-3	9953280	SM-G.653	40	1550	1530–1565	3–11	130	1	SLM-DFB/EM	ffs	0.1	−1/+2	8.2	ffs	PIN	26	−13	−1	1.0×10^{-12}
LR-1	9953280	SM-G.652	40	1310	1290–1330	17–22	130	1	SLM-DFB/DM	ffs	0.1	+4/+7	6	ffs	PIN/OA	OSNR 28	−19	−10	1.0×10^{-12}
LR-2a	9953280	SM-G.652	80	1550	1530–1565	11–22	1600	2	SLM-DFB/EM	ffs	0.1	−2/+2	10	ffs	PIN/OA	OSNR 30	−26	−9	1.0×10^{-12}
LR-2b	9953280	SM-G.652	80	1550	1530–1565	16–22	1600	2	SLM-DFB/EM	ffs	0.1	+10/+13	8.2	ffs	PIN	OSNR 30	−14	−3	1.0×10^{-12}
LR-2c	9953280	SM-G.652	80	1550	1530–1565	11–22	1600	2	SLM-DFB/EM	ffs	0.1	−2/+2	10	ffs	PIN/OA	OSNR 30	−26	−3	1.0×10^{-12}
LR-3	9953280	SM-G.653	80	1550	1530–1565	16–22	260	1	SLM-DFB/EM	ffs	0.1	+10/+13	8.2	ffs	PIN	OSNR 28	−13	−3	1.0×10^{-12}
VR-1	9953280	SM-G.652	60	1310	1290–1330	22–33	240	2	SLM-DFB/EM	ffs	0.1	+10/+13	10	ffs	PIN/OA	OSNR ffs	−24	−9	1.0×10^{-12}
VR-2a	9953280	SM-G.652	120	1550	1530–1565	22–33	2400	2	SLM-DFB/EM	ffs	0.1	+10/+13	10	ffs	PIN/OA	OSNR ffs	−25	−9	1.0×10^{-12}
VR-3	9953280	SM-G.653	120	1550	1530–1565	22–33	400	1	SLM-DFB/EM	ffs	0.1	+10/+13	8.2	ffs	PIN/OA	OSNR ffs	−24	−9	1.0×10^{-12}

FO standards groupings (left margin): 10G FO Telecom (G.g), STM-64 Telecom (G.691), OC-192 Telecom (G.2 CORE).

Table 1.4 Optical fiber telecommunication standards operating at the bit rate range of 40 Gb/s and fiber channel standards

FO standards	Nominal rate (Mb/s)	Recommendation	Application	Code	Bit rate (Mb/s)	Fiber	Distance (km)	Nominal WL (nm)	WL range (nm)	Attenuation range (dB)	CD$_{max}$ (ps/nm)	Modal BW (MHz km)	Penalty (dB)	Source	Linewidth RMS (nm)	SPD$_{max}$ (mW/MHz)	PWR range (dBm)	ER (dB)	SMSR (dB)	Detector	ESNR (dB10)	Sensitivity (dBm)	OVL (dBm)	BER
STM	40G	ITU-T G.959.1	Telecom 40G	VSR2000-3L1	39 813 120	SM-G.652	2	1310	1290–1330	3–6	6.6	NA	1	SLM-DFB/EM	ffs	ffs	+2/+5	10	35	PIN	ffs	−5	+2	1.0×10^{-12}
				VSR2000-3L2	39 813 120	SM-G.652	2	1550	1530–1565	0–6	40		1	SLM-DFB/EM	ffs	ffs	+1/+3	8.2	35	PIN	ffs	−6	+3	1.0×10^{-12}
				VSR2000-3L5	39 813 120	SM-G.655	2	1310	1290–1330	3–12	20		1	SLM-DFB/EM	ffs	ffs	+8/+10	10	35	PIN	ffs	−5	+2	1.0×10^{-12}
				VSR2000-3M1	39 813 120	SM-G.652	2	1550	1530–1565	3–12	6.6		1	SLM-DFB/EM	ffs	ffs	0/+3	7	35	PIN	ffs	−13	0	1.0×10^{-12}
				VSR2000-3M2	39 813 120	SM-G.655	2	1550	1530–1565	3–16	40		1	SLM-DFB/EM	ffs	ffs	0/+3	7	35	PIN	ffs	−17	0	1.0×10^{-12}
				VSR2000-3M5	39 813 120	SM-G.652	2	1550	ffs	ffs	20		1	SLM-DFB/EM	ffs	ffs	ffs	ffs	ffs	ffs	ffs	ffs	ffs	1.0×10^{-12}
				VSR2000-3H2	39 813 120	SM-G.652	2	1550	ffs	ffs	40		1	SLM-DFB/EM	ffs	ffs	ffs	ffs	ffs	ffs	ffs	ffs	ffs	1.0×10^{-12}
				VSR2000-3H5	39 813 120	SM-G.655	2	1550	ffs	ffs	20		1	SLM-DFB/EM	ffs	ffs	ffs	ffs	ffs	ffs	ffs	ffs	ffs	1.0×10^{-12}
		ITU-T G.691	Telecom	I-256.2	39 813 120	SM-G.652	25	1550	ffs	ffs	ffs		ffs	SLM-DFB/EM	ffs	ffs	ffs	ffs	ffs	ffs	ffs	ffs	ffs	1.0×10^{-12}
				S-256.2	39 813 120	SM-G.652	40	1550	ffs	ffs	ffs		ffs	SLM-DFB/EM	ffs	ffs	ffs	ffs	ffs	ffs	ffs	ffs	ffs	1.0×10^{-12}
				S-256.3	39 813 120	SM-G.653	40	1550	ffs	ffs	ffs		ffs	SLM-DFB/EM	ffs	ffs	ffs	ffs	ffs	ffs	ffs	ffs	ffs	1.0×10^{-12}
				L-256.2	39 813 120	SM-G.652	80	1550	ffs	ffs	ffs		ffs	SLM-DFB/EM	ffs	ffs	ffs	ffs	ffs	ffs	ffs	ffs	ffs	1.0×10^{-12}
				L-256.3	39 813 120	SM-G.653	80	1550	ffs	ffs	ffs		ffs	SLM-DFB/EM	ffs	ffs	ffs	ffs	ffs	ffs	ffs	ffs	ffs	1.0×10^{-12}

FO standards	Nominal rate (Mb/s)	Recommendation	Application	Code	Bit rate (Mb/s)	Fiber	Distance (m)	Nominal WL (nm)	WL range (nm)	Attenuation range (dB)	Modal BW (MHz km)	Penalty (dB)	Source	Linewidth RMS (nm)	Tx OMA min (µW)	Tx AVR range (dBm)	ER (dB)	SMSR (dB)	Detector	Rx OMA sen (µW)	Rx AVR sen (dBm)	Rx AVR ovl (dBm)	BER
1G FC	1G	FC-PI-R	Datacom/Storage	100-SM-LC-L	1062 5	SM-G.652	10 000	1310	1285–1345	0–8	NA	2	MLM-FP-VCSEL	3	174	−9.5/−3	9	NA	PIN	15	−20.2	−3	1.0×10^{-12}
				100-M5-SN-I	1062 5	MM-G.651	5000	850	770–860	0–4	500	3	MLM-FP-VCSEL	1	156	−10/0	9	NA	PIN	31	−17	0	1.0×10^{-12}
				100-M6-SN-I	1062 5	MM-62.5µ	3000	850	770–860	0–3	200	4	MLM-FP-VCSEL	1	156	−10/0	9	NA	PIN	31	−17	0	1.0×10^{-12}
2G FC	2G	FC-PI-R	Datacom/Storage	200-SM-LC-L	2125	SM-G.652	10 000	1310	1290–1340	0–8	NA	2	MLM-FP-VCSEL	2	150	−10.4/−3	10	NA	PIN	15	−20.4	−3	1.0×10^{-12}
				200-M5-SN-I	2125	MM-G.651	300	850	830–860	0–3	500	3	MLM-FP-VCSEL	0.85	196	−9.2/0	10	NA	PIN	49	−15.2	0	1.0×10^{-12}
				200-M6-SN-I	2125	MM-62.5µ	150 00	850	830–860	0–2	200	4	MLM-FP-VCSEL	−0.85	196	−9.2/0	10	NA	PIN	49	−15.2	0	1.0×10^{-12}
4G FC	4G	FC-PI-R	Datacom/Storage	400-SM-LC-L	4250	SM-G.652	10 000	1310	1265–1365	0–8	NA	2	SLM-DFB	<1 at −20 dB	290	−7.5/−3	10	NA	PIN	29	−17.5	−1	1.0×10^{-12}
				400-M5-SN-I	4250	MM-G.651	150 00	850	830–860	0–2	500	4	MLM-FP-VCSEL	0.85	247	−8.2/0	10	NA	PIN	61	−14.2	0	1.0×10^{-12}
				400-M6-SN-I	4250	MM-62.5µ	7000	850	830–860	0–2	200	4	MLM-FP-VCSEL	0.85	247	−8.2/0	10	NA	PIN	61	−14.2	0	1.0×10^{-12}

Table 1.5 Optical fiber datacommunication standards operating at the bit rate range of 10 Gb/s

FO standards	Nominal rate (Mb/s)	Recommendation	Application	Code	Bit rate (Mb/s)	Fiber	Distance (m)	Nominal WL (nm)	WL range (nm)	Power budget (dB)	Modal BW (MHz km)	Penalty (dB)	Source	Linewidth RMS (nm)	Tx OMA min (µW)	Tx AVR range (dBm)	ER (dB)	SMSR (dB)	Detector	Rx OMA sens (µW)	Rx AVR sens (dBm)	Rx AVR ovl (dBm)	BER
1 GbE	1 G	IEEE P802.3z/D5.0	SFP Datacom	1000BA SE-SX	1250	MM-62.5µ	220	850	770–860	7.5	160	5.1	MLM-FP-VCSEL	0.85	174	−9.5/0	9	NA	PIN	31	−17	0	1.0×10^{-12}
						MM-G.651	275	850	770–860	7.5	200	4.9	MLM-FP-VCSEL	0.85	174	−9.5/0	9	NA	PIN	31	−17	0	1.0×10^{-12}
							500				400	4.1											1.0×10^{-12}
							550				500	3.9											1.0×10^{-12}
				1000BA SE-LX	1250	MM-62.5µ	550	1310	1270–1355	7.5	500	5.1	MLM-FP-VCSEL	4	110	−11.5/−3	9	NA	PIN	20	−19	−3	1.0×10^{-12}
						MM-G.651	550	1310	1270–1355	7.5	500	5.1	MLM-FP-VCSEL	4	110	−11.5/−3	9	NA	PIN	20	−19	−3	1.0×10^{-12}
						SM-G.652	550	1310	1270–1355	8.0	500	3.4	MLM-FP-VCSEL	4	124	−11/−3	9	NA	PIN	20	−19	−3	1.0×10^{-12}
							5000				NA												1.0×10^{-12}
10 GbE	10 G	IEEE P802.3ae	XFP X2 XPAK XENPAK Datacom	10BA SE-SW	9953280	MM-62.5µ	26	850	840–860	7.3	160	5.7	MLM-FP-VCSEL	0.45	124	−7.3/−1	3	NA	PIN	68	−9.9	−1	1.0×10^{-12}
						MM-G.651	33				200	5.1											1.0×10^{-12}
							66				400	5.6											1.0×10^{-12}
							82				500	5.5											1.0×10^{-12}
							300				2000	4.7											1.0×10^{-12}
				10BA SE-SR	10312.50	MM-62.5µ	26	850	840–860	7.3	160	5.7	MLM-FP-VCSEL	0.45	124	−7.3/−1	3	NA	PIN	68	−9.9	−1	1.0×10^{-12}
						MM-G.651	33				200	5.6											1.0×10^{-12}
							66				400	5.6											1.0×10^{-12}
							82				500	5.5											1.0×10^{-12}
							300				2000	4.7											1.0×10^{-12}
				10BA SE-LW	9953280	SM-G.652	10000	1310	1260–1355	9.4	NA	3.2	SLM-DFB	NA	116	−8.2/+0.5	3.5	30	PIN	28	−14.4	0.5	1.0×10^{-12}
				10BA SE-LR	10312.50	SM-G.652	10000	1310	1260–1355	9.4	NA	3.2	SLM-DFB	NA	116	−8.2/+0.5	3.5	30	PIN	28	−14.4	0.5	1.0×10^{-12}
				10BA SE-EW	9953280	SM-G.652	30000	1550	1530–1565	15.0	NA	4.1	SLM-DFB	NA	226	−4.7/+4.0	3	30	PIN	17.5	−15.8	−1	1.0×10^{-12}
				10BA SE-ER	10312.50	SM-G.652	10000	1550	1530–1565	15.0	NA	4.1	SLM-DFB	NA	100	−8.2/+0.5	3	30	PIN	17.5	−15.8	−1	1.0×10^{-12}

Table 1.5 (*continued*)

FO standards	Nominal rate (Mb/s)	Recommendation	Application	Code	Bit rate (Mb/s)	Fiber	Distance (m)	Nominal WL (nm)	WL range (nm)	Power budget (dB)	Modal BW (MHz km)	Penalty (dB)	Source	Line-width RMS (nm)	Tx OMA min (µW)	Tx AVR range (dBm)	ER (dB)	SMSR (dB)	Detector	Rx OMA sens (µW)	Rx AVR sens (dBm)	Rx AVR ovl (dBm)	BER
				10GBA SE-LX4	3 125	MM-62.5µ	300	1310-L0 1310-L1 1310-L2 1310-L3	1269.0–1282.4 1293.5–1306.9 1318.0–1331.4 1342.5–1355.9	7.5	500	5.5	MLM-FP-VCSEL	0.62	682	−0.5/+5.5	3.5	NA	PIN	28.5	−14.25	−0.5	1.0×10^{-12} 1.0×10^{-12} 1.0×10^{-12} 1.0×10^{-12}
							240	1310-L0 1310-L1 1310-L2 1310-L3	1269.0–1282.4 1293.5–1306.9 1318.0–1331.4 1342.5–1355.9	7.5	400	5.6	MLM-FP-VCSEL	0.62	682	−0.5/+5.5	3.5	NA	PIN	28.5	−14.25	−0.5	1.0×10^{-12} 1.0×10^{-12} 1.0×10^{-12} 1.0×10^{-12}
						MM-G.651	300	1310-L0 1310-L1 1310-L2 1310-L3	1269.0–1282.4 1293.5–1306.9 1318.0–1331.4 1342.5–1355.9	7.5	500	5.5	MLM-FP-VCSEL	0.62	682	−0.5/+5.5	3.5	NA	PIN	28.5	−14.25	−0.5	1.0×10^{-12} 1.0×10^{-12} 1.0×10^{-12} 1.0×10^{-12}
						SM-G.652	10000	1310-L0 1310-L1 1310-L2 1310-L3	1269.0–1282.4 1293.5–1306.9 1318.0–1331.4 1342.5–1355.9	8.2	NA	2.0	SLM-DFB	0.62	682	−0.5/+5.5	3.5	NA	PIN	28.5	−14.45	−0.5	1.0×10^{-12} 1.0×10^{-12} 1.0×10^{-12} 1.0×10^{-12}
				10BA SE-LRM	10 312.50	MM-62.5µ	300 300 300	1310	1260–1385	8.5	500 500 500	6.5 6.5 6.5	MLM-FP-VCSEL-DFB	4	355	−6.5/+0.5	3.5	NA	PIN	50	−17	−1	1.0×10^{-12} 1.0×10^{-12} 1.0×10^{-12}
						MM-G.651	240 300				400 500	6.5 6.5											1.0×10^{-12} 1.0×10^{-12}

distributed feedback (DFB) lasers are all recommended due to compact packaging, yield and low cost. On the receiver side, receptacle PIN detectors are highly recommended.

4. Use standard MMF optical connector technology, avoiding any special alignment tolerance requirements.
5. Reduce module power consumption as much as possible in order to be compliant with next-generation higher-density low-profile optical interconnect modules.

State-of-the-art EDC designed using low-cost, high-speed, low-power and high-density CMOS IC technology can accommodate moderate optical pulse distortion, due to insufficient MMF bandwidth. However, OMF, even though it has not even if it been demonstrated to be fully capable of behaving as the outstanding solution due to many layout-dependent problems, could mitigate multimode fiber bandwidth limitation, thus reducing at least the EDC design complexity.

At the present time, EDC design based on high-speed CMOS technology is targeted at a compensation distance of 300 m over a legacy multimode fiber link. Longer distances result in a compensation effect that is not predictable, excessive design complexity and high power consumption. In conjunction with EDC, OMF or PAM-4 could even be the proper 'link extender', used to reach longer distances with stable results.

1.8 Optical Fiber Transmission Standards

Optical fiber transmission protocols and specifications are carefully controlled by several Standards Committees. Depending on the target application, optical fiber transmission systems are addressed for telecommunication and datacommunication areas. Different specifications characterize these two fields: privileged performance and reliability in the first case while stressing engineering solutions for a high-volume and low-cost market in the second case. The same data transmission speed demands quite different laser sources and detection technologies. Long-reach requirements in telecommunications very often need several hundred kilometers of single-mode fiber link, with large use of optical amplifier and dense wavelength division multiplexing (DWDM) technologies. For the large distribution of multigigabit data transmission implementation of legacy multimode fiber deployed in the 1980s and 1990s is required with very sensible bandwidth limitations. This situation sets a great engineering challenge in the local area distribution market. According to these specific business areas, several standards have been proposed. Tables 1.1 to 1.5 report the most relevant optical fiber standards, including the principal parameters for the fiber medium, the optical receiver and the optical transmitter. Major standard committees included are the following:

1. International Telecommunication Union, ITU-T G.XXX
2. Bellcore–Telcordia, GR-253-CORE
3. Fiber Channel, FC-PI
4. IEEE802.3ae, Gigabit Ethernet